Journal of Mathematical Economics 107 (2023) 102852

Contents lists available at ScienceDirect

Journal of Mathematical Economics

journal homepage: www.elsevier.com/locate/jmateco

Can one hear the shape of a target zone?☆

Jean-Louis Arcand [a,d,e,f], Shekhar Hari Kumar [a], Max-Olivier Hongler [b], Daniele Rinaldo [c,*]

[a] Graduate Institute of International and Development Studies, Geneva, Switzerland
[b] École Polytechnique Fédérale, Lausanne, Switzerland
[c] University of Exeter Business School and Land, Environment, Economics and Policy Institute, Exeter, United Kingdom
[d] FERDI, Clermont-Ferrand, France
[e] Global Development Network, New Delhi, India
[f] UM6P, Rabat, Morocco

ARTICLE INFO

Article history:
Received 14 October 2021
Received in revised form 1 May 2023
Accepted 1 May 2023
Available online 22 May 2023
Manuscript handled by Editor Andrés Carvajal

Keywords:
Exchange rate target zones
Non-stationary exchange rate dynamics
Reflected stochastic differential equations
Dynamic mean-preserving spreads
Spectral gap
Regime shifts

ABSTRACT

We develop an exchange rate target zone model with finite exit time and non-Gaussian tails. We show how the tails are a consequence of time-varying investor risk aversion, which generates mean-preserving spreads in the fundamental distribution. We solve explicitly for stationary and non-stationary exchange rate paths, and show how both depend continuously on the distance to the exit time and the target zone bands. This enables us to show how central bank intervention is endogenous to both the distance of the fundamental to the band and the underlying risk. We discuss how the feasibility of the target zone is shaped by the set horizon and the degree of underlying risk, and we determine a minimum time at which the required parity can be reached. We prove that increases in risk beyond a certain threshold can yield endogenous regime shifts where the "honeymoon effects" vanish and the target zone cannot be feasibly maintained. None of these results can be obtained by means of the standard Gaussian or affine models. Numerical simulations allow us to recover all the exchange rate densities established in the target zone literature. The generality of our framework has important policy implications for modern target zone arrangements.

1. Introduction

The exchange rate target zone literature, pioneered by Krugman (1991), highlights the role that market expectations concerning fundamentals play in shaping exchange rate movements and is based on a stochastic flexible price monetary model in continuous time. Given its assumptions of perfect credibility and Gaussian fluctuations in the fundamental, it implies that central bankers need only intervene marginally at the bounds of the target zone or allow honeymoon effects to automatically stabilize the exchange rate. The European Monetary System (EMS) and the Exchange Rate Mechanism (ERM), which existed from 1979 until participating countries adopted the Euro in 1999, provided a natural test bed for this theory. The target zone model has provided the intellectual justification for the choice of a nominal anchor for countries transitioning to a monetary union.

While the use of target zone exchange rate regimes became less common after the 1990s, their practice continues to this day, with the ERM-II target zone mechanism being an intermediate step to Euro adoption for new member states.[1] It is likely that future new member states will also participate in the ERM process, making target zone modeling of current relevance. In its review of the ERM-II, the European Central Bank (ECB) notes that participation in the target zone may involve both positive and negative regime shifts driven by changing expectations and economic incentives of international and local investors, as well as those of local policy authorities (Dorrucci et al., 2020). This mechanism can be observed in the ERM-II experiences of countries around the Great Financial Crisis (GFC). ERM-II countries experienced much higher capital flow volatility and associated credit boom-bust cycles as compared to similar countries that had a peg to the Euro but did not join the ERM. Entering a target zone with a "credible" commitment to join the Euro has led to a shift in expectations about country (currency) risk, which drifted towards converging with the European Monetary Union. The relaxation of the external borrowing constraint through the ERM process generated a capital flow boom (Fornaro, 2020). However, this process of monetary integration is subject to downside risks as

☆ The authors thank Joshua Aizenman, Ugo Panizza, Didier Sornette and Cédric Tille for their precious insights.

* Corresponding author.
E-mail address: d.rinaldo@exeter.ac.uk (D. Rinaldo).

[1] As of writing this paper, Bulgaria and Denmark are in the ERM-II target-zone. Bulgaria intends to adopt the Euro whereas Denmark has a special opt-out clause from Euro adoption.

https://doi.org/10.1016/j.jmateco.2023.102852

well, as unanticipated changes in global investor risk aversion may lead to destabilizing capital flow reversals.

Existing attempts at modeling fundamental risk in a target zone involve either Gaussian fluctuations, the addition of ad-hoc jumps, or deviations from rational expectations. These features are unable to capture the risk-driven regime shift dynamics associated with target zone mechanisms such as the ERM-II which involves the finite time based adoption of a larger target currency. In this paper, we study the dynamics of an exchange rate target zone with a finite-time exit to a target currency, whilst accounting formally for the risk generated by the convergence process. We show how this source of risk destabilizes the exchange rate fundamentals and generates extra pressure to move towards the boundary. We do so by assuming that the risk aversion of foreign investors is subject to risk-on and risk-off shocks, which generate a country-risk premium in the uncovered interest rate parity condition via a sudden bonanza or sudden stop of capital flows during the target zone process. We show how this mechanism introduces the dynamic equivalent of mean-preserving spreads in the fundamental process, which generates non-Gaussian tails in the exchange rate distribution. We are able to solve analytically the partial differential equation with reflecting boundaries associated with the exchange rate path within the target zone, by means of an eigenfunction expansion and Sturm–Liouville theory. We make four main contributions to the literature.

First, we formally document the presence of "soft" boundaries, which determine central bank interventions by means of the exchange rate's distance to the bands as well as the intensity of external risk. We find that the underlying dynamics are similar to the phenomena famously described by Kac (1966), who studied whether one could *"hear the shape of a drum"* if all the eigenvalues of the corresponding eigenvalue problem are known. In our framework, the shape of a target zone can indeed be "heard", when the exchange rate is pushed to the sides of the target band by an additional external destabilizing force: intuitively, this corresponds to the acoustic difference between striking a tense membrane (large shifts in risk aversion) versus a loose one. External risk is not simply subsumed in the variance of idiosyncratic fluctuations in the fundamental, but emerges as a non-Gaussian, destabilizing force. The resulting mean-preserving spreads allow one to effectively endogenize the bands, providing an explanation for the existence of smaller *de facto* bands within larger *de jure* target bands, as well as the possibility of marginal and intra-marginal interventions in a target zone without assuming a specific foreign exchange intervention strategy. This mechanism has been shown empirically to exist and has been described heuristically (Lundbergh and Teräsvirta, 2006; Bessec, 2003), but was heretofore not formalized precisely.

Our second main contribution lies in our being able to characterize the minimum time for which a target zone needs to be maintained for the home currency to successfully exit to the target currency. We do so by studying the relaxation time of the exchange rate process, which is the inverse of the distance between 0 and the smallest eigenvalue in the spectrum, a quantity also known as the spectral gap. The relaxation time is the minimum required time for agents to "feel" the first effects of the home central bank's actions aimed at reducing fluctuations of the exchange rate. It is also the minimum time necessary for agents to update their priors accurately, generating self-fulfilling expectations that create the honeymoon effect for future central bank actions. This result allows us to characterize precisely the *feasibility* of a target zone, which corresponds to the central bank being able to reach the set central parity with the agreed bands at the chosen time horizon. We characterize analytically the minimum required time necessary for the parity to be reached: any shorter time horizon chosen by the central bank would be unfeasible. Our model further shows that it is mandatory to study non-stationary dynamics in order to determine whether the chosen horizon is feasible. In contrast, existing models assume away the problem by positing perfect feasibility and stationary dynamics.

Third, we show how large shocks to investor risk aversion, leading to proportional increases in risk and non-Gaussian tails in the fundamental distribution, can potentially yield a regime shift in the spectrum once a certain risk threshold is crossed. This shift does not allow anymore honeymoon effects to arise around the target zone bands, since the increase in risk destabilizes the exchange rate dynamics to the point that smooth-fitting procedures around the band cannot be applied by central bank interventions and the target zone becomes untenable. Beyond a critical threshold of risk, therefore, the target zone effectively cannot exist, and we show how this threshold is bounded below by the reciprocal of the target zone bandwidth. This implies that the central bank has to widen the target zone bands in order to maintain control of the exchange rate. This result can only be explained in standard models by explicitly assuming *ad hoc* endogenous devaluation risk.

Finally, our framework is very general: we are able to show how the model can fit a wide range of scenarios regarding feasibility and control. We are able to replicate by Monte Carlo simulations the various exchange rate densities predicted by the established target zone literature.

The paper is organized as follows. Section 2 provides a brief review of the existing literature. Section 3 presents the model and its solution. Section 4 discusses the connection between risk, target zone width and feasibility, presents the emergence of regime shifts once a critical threshold of risk is reached and shows the generality of our framework via numerical simulations. Section 5 discusses the policy implications of our model and its real-world applications, while Section 6 concludes and presents an agenda for future research.

2. Existing literature

The literature begins with the seminal paper by Krugman (1991), which hinges on the assumptions of perfect credibility and Gaussian fluctuations in the fundamental process, giving rise to an U-shaped distribution of the exchange rate and a negative relationship between the interest rate differential and exchange rate volatility. The exchange rate is therefore expected to spend most of its time near the bands of the zone, and due to the honeymoon effect the central bank only has to intervene marginally at the bands. There has been scant empirical support for this framework, however. In particular, both the implied U-shaped distribution and the negative correlation between the exchange rate and the interest rate differential have found little counterpart in the data, as shown by Mathieson et al. (1991), Meese and Rose (1991) and Svensson (1991).

This result led to the development of the so-called second-generation models, starting with Bertola and Caballero (1992) and Bertola and Svensson (1993), up to Tristani (1994) and Werner (1995) who study endogenous realignment risk. Second-generation models focus on allowing the fundamental process to be controlled intramarginally, thus generating a hump-shaped distribution where the exchange rate spends most of its time around central parity. Dumas and Delgado (1992) show that the honeymoon effects are considerably weakened when central banks intervene intramarginally. Serrat (2000) generalizes the target zone framework to a multilateral setting, and shows how spillovers from third-country interventions can increase conditional volatilities compared to free-float regimes. Bekaert and Gray (1998) and Lundbergh and Teräsvirta (2006) test the

implications of the second-generation models, and find mixed evidence with a slight tendency towards the intramarginal interventions hypothesis. Ajevskis (2011) extends the basic target zone model to a finite termination time setting while maintaining the other assumptions of the original model.

Recently, Studer-Suter and Janssen (2017) and Lera and Sornette (2016, 2018 and 2019) find empirical evidence for the target zone model for the EUR/CHF floor target zone set by the Swiss National Bank between 2011 and 2015, the latter mapping the Krugman model to the option chain. In particular, Lera and Sornette (2015) show how the standard model can hold in specific cases, such as the EUR/CHF target zone, because of a sustained pressure that continuously pushes the exchange rate closer to the bounds of the target zone, which the central bank tries to counteract. Such pressure is a common feature of target zone arrangements: Rey (2015) famously argued that the global financial cycles stemming from the United States generate additional risks for central banks targeting a nominal anchor. Furthermore, Gopinath and Stein (2019) and Kalemli-Özcan (2019) show how US monetary policy shocks can affect the exchange rate of a country with minimal USD exposure because of the dominant nature of the USD as a trade currency, implying that the alignment process generated by a target zone naturally generates additional risk.

3. The model

In this paper we want to characterize a modern target zone mechanism in which the fundamental process can be destabilized by external risk factors, generating thick non-Gaussian tails in its distribution. Inclusion of these characteristics in the analysis is made necessary by the presence of risk-averse investors who have time varying risk aversion modulated by the global financial cycle. Entering a target zone increases the capital market integration of the country in question which exposes countries' fundamentals to an increased share of global and regional risk factors.[2]

3.1. Risk aversion shocks

The target zone framework depends critically on the uncovered interest rate parity (UIP) condition, with the currency in the target zone converging to the target nominal interest rate at time of exit to the currency union. The UIP condition requires risk-neutral preferences: this is usually not the case when we are considering real-world situations, as investors are generally risk-averse. risk aversion, however, is likely to change over time due to risk-on and risk-off shocks arising from global financial conditions. Let us consider that investors face a standard problem of bond consumption with concave utility $U(c_t)$ with discount factor γ. At any time t, the agent's coefficient of relative risk aversion $-cU''/U'$ at time $t+1$ can be incremented by an amount $\lambda \in \mathbb{R}^+$ which can be either negative (risk-on) or positive (risk-off) with equal probability, yielding a new utility function $\bar{U}$.[3]

This implies that the asset pricing kernel (the stochastic discount factor) will be given by

$$\gamma \frac{\bar{U}'(c_{t+1})}{U'(c_t)} = \gamma \frac{U'(c_{t+1})}{U'(c_t)} \Delta U'(c_{t+1}) = M_t \Delta U'(c_{t+1}),$$

where M_t is the pricing kernel without the change in risk aversion and $\Delta U'(c_{t+1})$ is the change in curvature of the utility function due to the change in risk aversion. Note that this last term is also a random variable. More generally, if consumption of bonds is at two discrete time points but their evolution is continuous, this extra term is equivalent to the Radon-Nikodým derivative for the change of measure between the densities generated by the differently curved utility functions. The investors' pricing kernel is therefore

$$\gamma \frac{\bar{U}'(c_{t+1})}{U'(c_t)} = \frac{d\mathbb{Q}}{d\mathbb{P}} \frac{d\tilde{\mathbb{Q}}}{d\mathbb{Q}},$$

where $\mathbb{Q}$ is the foreign martingale measure of the home bond under the original measure $\mathbb{P}$, and $\tilde{\mathbb{Q}}$ is the foreign martingale measure under the new utility function. The UIP condition is then given by

$$\mathbb{E}\{dX_t\} \frac{(1+i_t^*)}{(1+i_t)} = \frac{d\mathbb{Q}}{d\tilde{\mathbb{Q}}}, \tag{1}$$

where $\mathbb{E}\{dX_t\}$ is the expectation of the log exchange rate conditional on information available up to t and i^*, i are respectively the foreign and domestic interest rates. In (1) the excess returns required to complete the no-arbitrage condition decrease with the investors' risk aversion, since $\frac{d\mathbb{Q}}{d\tilde{\mathbb{Q}}}$ increases with a realization of $+\lambda$ (decreased risk aversion) and vice versa.

Eq. (1) is a modified UIP condition where the time-varying risk premium is dependent on the change in investor risk aversion. If we assume again log-normality of the foreign bond, since the change in risk aversion is equally likely on each side (each $\pm\lambda$ is realized with probability 0.5), it is easily shown that the new measure after the change in risk aversion is given by a Gaussian density identical to the pricing kernel without the curvature change, and an oscillating term that takes values $\pm\lambda$ with equal probability, represented by a Bernoulli variable. We note that the overall new measure $d\tilde{\mathbb{Q}}/d\mathbb{P}$ is still a martingale but is not Gaussian, even assuming an underlying (log) Normal distribution: the oscillation of the change in curvature of the utility function generates an extra term

$$\frac{d\tilde{\mathbb{Q}}}{d\mathbb{Q}} = \frac{1}{2}\left(e^{-(x+\lambda)^2/2} + e^{-(x-\lambda)^2/2}\right), \tag{2}$$

which is precisely the perturbation of a Gaussian process by means of a Bernoulli variable in the drift. We therefore have a risk premium that is dependent on the equiprobable oscillation $\pm\lambda$ of investors' risk aversion.

3.2. Dynamic mean-preserving spreads and exchange rate target zones

Let us now include (1) and (2) in the exchange rate dynamics. As is standard in the literature, the fundamental process for the (log) exchange rate f_t evolves according to $df_t = dv_t + dm_t$, where v_t is a money demand shock (velocity) m_t is money supply, usually assumed to be controlled by the central bank. As shown in Appendix A, the risk premia from the modified UIP condition (1) can be included in the velocity of a monetary model of exchange rate determination, and we can write the fundamental process as the stochastic differential equation

$$df_t = \lambda \mathcal{B} dt + \sigma dW_t, \qquad f_{t=0} = f_0, \tag{3}$$

[2] Fornaro (2020) finds that entering a currency union increases financial integration between member states. This is due to reduction of currency risk and the associated easing of external borrowing constraints, driven in part by loss of national monetary and fiscal autonomy. A target zone setting is a *quasi-currency union* with the chosen target zone band representing the range of expected fluctuations. Evidence from New Member States suggests that the magnitude of capital flows received may be very high even if the member state does not enter the target zone process for adopting the Euro (Mitra, 2011). This may be considered analogous to the index effects documented by Hau et al. (2010) for emerging market currencies.

[3] This framework is equivalent to assuming heterogeneous investors, identical in everything except in risk aversion, where between t and $t+1$ each changes her own risk aversion to a specific amount, and the resulting $\pm\lambda$ is the aggregate overall change in the representative utility function.

in the probability space $(\mathbb{R}, \mathcal{F}, P)$ where dW_t is the standard Brownian motion with diffusion parameter σ and $\mathcal{B}$ is a Bernoulli random variable that takes on the values $\{-1, 1\}$ each with probability 0.5 and $\lambda \in \mathbb{R}^+$. Without any loss of generality, (3) can be rescaled as

$$df_t = \beta \mathcal{B} dt + dW_t, \tag{4}$$

where $\beta = \lambda/\sigma^2$ is the rescaled risk parameter. The stochastic process (4) driving the fundamental is the dynamic equivalent of a mean-preserving spread, and has been studied by Arcand et al. (2020). Risk aversion shocks in the velocity, therefore, cause an increase in risk in the fundamental that push probability away from the mean and generate non-Gaussian tails, whilst leaving the systematic average unchanged.

As seen in Eqs. (1) and (2), such shocks cannot be represented by Gaussian fluctuations, and we prove this formally in Appendix D. This also allows us to precisely characterize the interplay of diffusive fluctuations (variance) and destabilizing forces[4] (risk, via changes in investor risk aversion): the pressure that external risk causes that pushes the exchange rate towards the bounds is counteracted by the central bank's efforts to maintain the fundamental fluctuating around its mean. This is precisely what is observed by Lera and Sornette (2015), who show that this sustained pressure stemmed from the Swiss Franc being used as a safe asset in the middle of the European crisis.

By the definition of a target zone, the central bank requires the fundamental process to remain bounded within a set interval $[\underline{f}, \bar{f}] \in \mathbb{R}$. By adjusting money supply, the central bank regulates the fundamental process within this interval, also known as the target band. As shown in Appendix A, the equation for the log-exchange rate X_t under the modified UIP condition (1) in the interval $[\underline{f}, \bar{f}]$ can therefore be written as the regulated stochastic differential equation

$$X_t = f_t + \frac{1}{\alpha}\mathbb{E}\{dX_t\} \qquad f_t \in [\underline{f}, \bar{f}] \ \ \forall t \in [0, T], \tag{5}$$

where f_t evolves according to (4), equipped with the reflecting ("smooth pasting") boundary conditions

$$\partial_f X_t \mid_{f=\underline{f}} = \partial_f X_t \mid_{f=\bar{f}} = 0. \tag{6}$$

At a fixed time T the spot exchange rate is set to exit the target zone and match the target fundamentals. We are interested in the exchange rate dynamics generated by (5) throughout the time interval $[0, T]$, and therefore explicitly allow time-dependent dynamics $X_t = X(t, f_t)$ and study non-stationary behavior. The term $1/\alpha$, with $0 < \alpha < 1$ is the absolute value of the semi-elasticity of money with respect to the nominal interest rate. As this quantity is always greater than unity, we interpret it as a frequency (i.e. 1/[time unit]) which modulates the size of the forward-looking time window. For simplicity of exposition, we focus our attention on target zones that are symmetric around 0 of the form $[-\bar{f}, \bar{f}]$, although all our results hold for general bounds. We can now state the main result of the paper.

Proposition 1. *The solution of the stochastic differential equation (5) reflected via (6) in the bounded domain $[0, T] \times [\underline{f}, \bar{f}] \to \mathbb{R}$ is given by the process*

$$X(t, f) = X^*(t, f) + X_S(f), \tag{7}$$

which is the sum of stationary and non-stationary solutions. The stationary solution is given by

$$X_S(f) = \cosh(\beta f)^{-1} \left[A\mathcal{Y}_1(f) + B\mathcal{Y}_2(f) + \mathcal{Y}_P(f)\right], \tag{8}$$

where we have:

$$\mathcal{Y}_1(f) = \exp\left(+\sqrt{\left[\beta^2 + 2\alpha\right]} f\right),$$

$$\mathcal{Y}_2(f) = \exp\left(-\sqrt{\left[\beta^2 + 2\alpha\right]} f\right),$$

$$\mathcal{Y}_P(f) = \frac{[\alpha f \cosh(\beta f) + \beta \sinh(\beta f)]}{\alpha}$$

and the constants A, B are obtained by smooth-fitting at the boundaries

$$\partial_f X_S(f) \mid_{f=\underline{f}} = \partial_f X_S(f) \mid_{f=\bar{f}} = 0. \tag{9}$$

The non-stationary solution is obtained by means of an eigenfunction expansion and is given by

$$X^*(t, f) = \cosh(\beta f)^{-1} \sum_{k=1}^{\infty} c_k \exp\left[-(\Omega_k^2 + \rho)(T - t)\right] \times \sin\left(\sqrt{2}\Omega_k f\right) \tag{10}$$

with $\rho = \frac{\beta^2}{2} + \alpha$ and Fourier coefficients given by

$$c_k = -\frac{1}{\bar{f}} \int_{-\bar{f}}^{+\bar{f}} X_S(f) \sin\left(\sqrt{2}\Omega_k f\right) df.$$

This solution is defined over a complete set of real eigenvalues $\{\Omega_1, \ldots, \Omega_k, \ldots\}$, $k = \mathbb{N}^+$ that solve

$$\sqrt{2}\Omega_k \cot\left(\Omega_k \bar{f}\right) - \beta \tanh(\beta \bar{f}) = 0, \qquad \forall k \in \mathbb{N}^+ \tag{11}$$

and span the discrete spectrum $\Omega := \left\{\Omega_k(\beta, \bar{f})\right\}$.

Proof. See Appendix B.

To see how the results are unaffected by both the band choice and its symmetry around 0, notice that the bounds enter the particular solution only via the scalar quantities A and B, and in the general solution via the integration limits of the Fourier coefficients. An illustration of the stationary solution (8) is presented in Fig. 1, which also shows how an increase in risk β in the fundamental prompts the (stationary) exchange rate to behave more independently of the dynamics of the fundamental. At high levels of β, the exchange rate dynamics are driven mostly by the risk and depend less on fundamentals, especially around the bounds, as represented by the steepening of the central slope. In this figure, $\bar{f} = 10\%$ and we assume a quasi-daily time step for the expectation $\alpha = 0.8$. Our parameterization of $\alpha = 0.8$ corresponds to a case of fast agent updating, which is similar to the case studied by Ferreira et al. (2019) and Coibion and Gorodnichenko (2015). Changing the α to a lower fundamental updating frequency will reduce the sensitivity of the exchange rate to the fundamentals.

For any $k \in \mathbb{N}^+$, the corresponding $\Omega_k(\beta, \bar{f})$ solves (11), and has to be calculated numerically. For a general $\beta > 0$, one observes that the successive eigenvalues are not evenly spaced, and display a distance which decreases in k. The spectrum is controlled by the width of the target zone $\bar{f}$: the wider the band, the smaller the separation. The spectrum and its relationship with the target band size are illustrated in Fig. 2. Observe also that in the limit $\beta = 0$, one straightforwardly verifies that from Eq. (11) one obtains the evenly spaced set $\Omega_k(0, \bar{f}) = (2k + 1)\frac{\pi}{2\bar{f}}$.

3.3. Can one hear the shape of a target zone?

When $t = T$, from Eq. (10), by construction of the Fourier coefficients c_k, we have $X^*(T, f) = -X_S(f)$ and so $X(T, f) = X^*(T, f) + X_S(f) = 0$ thus reaching the required fixed parity.

[4] The term $\beta\mathcal{B}$ is indeed a force, being the derivative of the probabilistic potential of the process f_t.

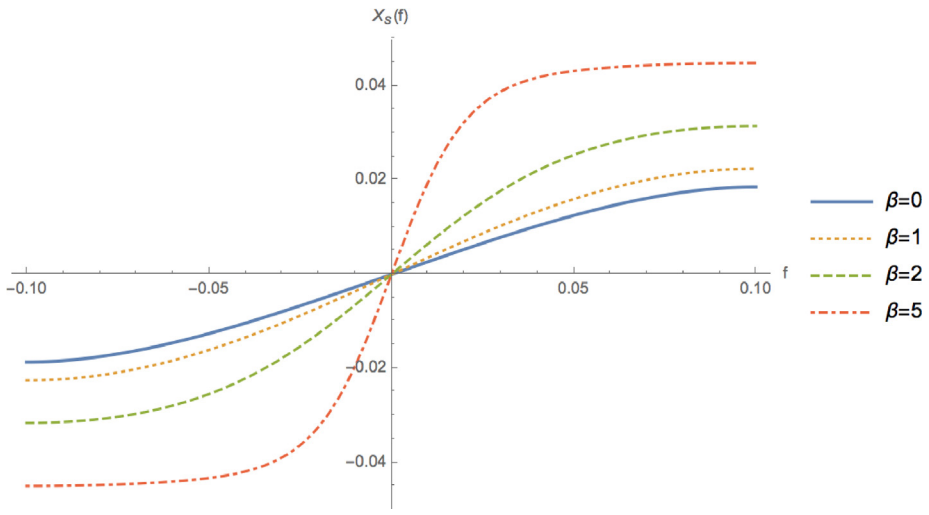

Fig. 1. Effect of varying β on stationary exchange rate dynamics.

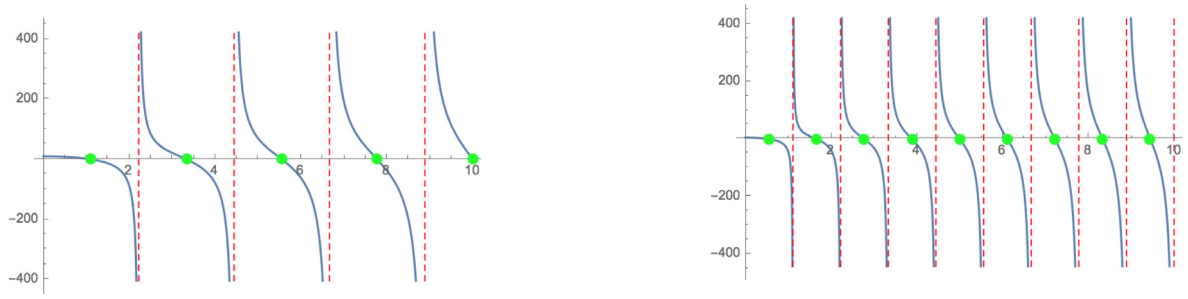

Fig. 2. Target zone band and spectrum. Graphical illustration of the solution of Eq. (11), showing the effect of varying $\bar{f}$ on the spectrum Ω_k.

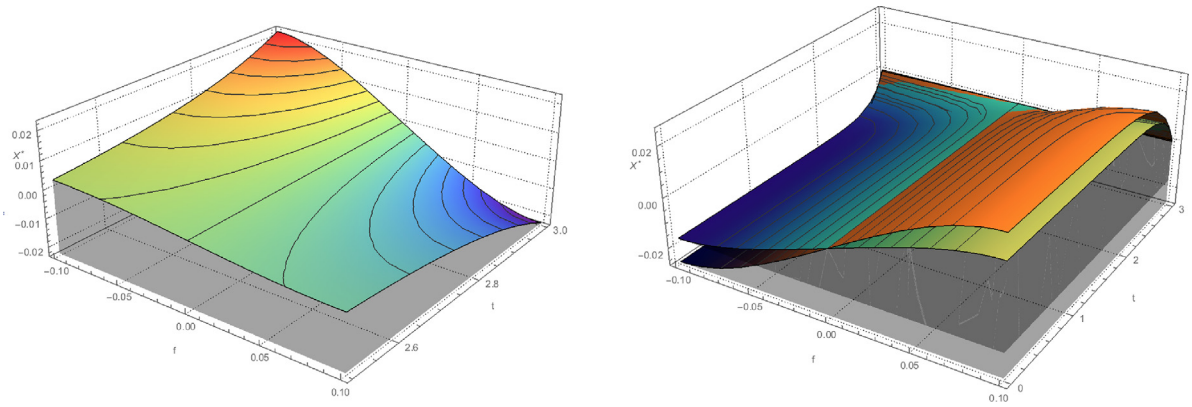

Fig. 3. Transient dynamics. This figure shows the evolution of $X(T-t, f)$ of the non-stationary dynamics in the target zone. The left panel shows the behavior of the time-dependent part: we assume a target zone which has been set to $T = 3$ years, with $\beta = 1$ for a given set of fundamentals. For the sake of visualization we truncate the figure towards the end of the target zone. The right panel shows the full dynamics for an increase in risk. Here we have assumed a target band symmetric around zero, i.e. $\bar{f} = 10\% = -\underline{f}$. We also assume $\alpha = 0.8$. We truncate the eigenfunction expansion at 50. The second panel illustrates the change in dynamics from $\beta = 0$ (Gaussian) to $\beta = 5$.

An illustration of the non-stationary exchange rate dynamics, as well as the overall transition dynamics throughout the time interval $[0, T]$, is presented in Fig. 3. The solution allows one to express the movements of the exchange rate via a weighted sum of its stationary behavior, its distance to the exit time and the distance between its value at any time t and the target band. The eigenvalues modulate the frequency of both fundamental and exchange rate movements within the band. The Fourier coefficients c_k represent the impact of the size of the target band in the overall dynamics, via their weight on the infinite series of frequency components (the "harmonics" of the exchange rate path). Loosely speaking, this formulation of the solution allows one to describe the sensitivity of the exchange rate to the distance to the target band. Once the spectrum and the eigenfunctions are

known, as famously asked by Kac (1966), *"if one had perfect pitch"*, one would be able to "hear" the shape of the target zone. Indeed, the time-independent part of the problem is a one-dimensional Neumann problem on the boundary $\partial D = [\underline{f}, \bar{f}]$

$$\begin{cases} \Delta f + \Omega f = 0 \\ \nabla f|_{\partial D} = 0, \end{cases}$$

which is exactly the problem of finding the overtones on a vibrating surface.

This formulation of the solution allows us to uncover the unique nature of the smooth-pasting conditions: the exchange rate process is not reflected at the bounds in the probabilistic sense, since this would have been modeled as a zero derivative condition on the transition probability density function. The eigenfunction expansion shows that in a target zone there exist "soft" boundaries, where the central bank interventions are determined by the interplay of the distance of the exchange rate to the bounds as well as the tendency of the fundamental to hit them (the risk). This allows us to "endogenize" the bands: because of $\mathbb{E}\{dX_t\}$ in the exchange rate Eq. (5), we have a second-order term which allows us to solve the equation in its Sturm–Liouville form. The Fourier coefficients in Proposition 1 modulate the sensitivity of the exchange rate to the distance to the band, allowing for the central bank to intervene whenever the fundamental is felt to be approaching the bounds.

This mechanism is a direct translation of how much the fundamental tends to escape and how much the central bank needs to intervene marginally or intramarginally: it is a direct consequence of the presence of expectations in the exchange rate equation. In other words, the higher the tendency to hit the bounds, the greater is the likelihood that the central bank will actually intervene intramarginally, with increasingly less weight placed on the actual position of the fundamental within the band. There exist therefore both *de jure* and *de facto* bands, which is a feature of target zones observed empirically by Lundbergh and Teräsvirta (2006): if the *de jure* band is large, expectations over the magnitude of risk react to a narrower *de facto* band. This is a phenomenon commonly observed in most ERM countries but not yet formalized.[5]

4. Feasibility, regime shifts and numerical simulations

In this section we discuss the key contributions of our framework: the role of the spectral gap in determining target zone feasibility, the characterization of the minimum feasible time to exit via the relaxation time of the exchange rate process, and how the fundamental risk can generate regime shifts that make honeymoon effects unobtainable. Furthermore, via numerical simulations we show how our model replicates the different exchange rate densities described in the established literature.

4.1. Target zone feasibility and the spectral gap

Let us begin by studying the interplay between the risk parameter β, the size of the target band $[-\bar{f}, +\bar{f}]$ and the time horizon T at which one reaches the target zone. We first note that at the initial time $t = 0$, from Eq. (10) we have $X^*(0, f) \approx 0$ and therefore $X(0, f) = X^*(0, f) + X_S(f) \approx X_S(f)$. Since $\Omega_1(\beta, \bar{f}) < \Omega_2(\beta, \bar{f}) < \cdots$, one can approximately write:

$$X(T, f) \simeq X_S(f) + \mathcal{O}\left(e^{-(\Omega_1^2+\rho)T}\right).$$

While for the exact solution we should have $X(T, f) = X_S(f)$, one sees immediately that $X(T - t, f) = X_S(f) + X^*(T - t, f)$ with $X^*(T - t, f)$ given by Eq. (10) nearly matches the exact solution, provided we have an horizon interval $T \gtrsim t_{\text{relax}}$ where $t_{\text{relax}} := \left(\Omega_1^2 + \rho\right)^{-1}$ is the characteristic relaxation time of the exchange rate process. This provides a validity range for the non-stationary dynamics given by the expansion of Eq. (10).

Hence, at time $t = 0$, the required initial probability law $X_S(f)$ is reached only for a large enough time horizon $T \gtrsim t_{\text{relax}}$. This now enables us to link the non-stationary dynamics of $X^*(t, f)$ to the **feasibility** of the target zone: the relaxation time τ_{relax} determines the *minimum time interval* for which a feasible target zone may be maintained. The larger β (the risk of the fundamental, stemming from larger shifts in agents' risk aversion), the greater is the tendency of the fundamental to escape from its mean; the authorities need therefore to maintain the target zone for a longer minimum duration. An increase in risk, for a given $\bar{f}$, implies that the target zone would have to be set for a longer horizon T to be feasible. Alternatively, for a given risk β, an increase of the target zone width $\bar{f}$, requires a longer minimal T implementation to ensure the overall feasibility of the policy. In other words, the central bank has to impose that the time horizon T is at least as large as the relaxation time t_{relax}.

An intuitive interpretation of the relaxation time in this framework is to understand t_{relax} as the characteristic elapsed time required to "feel" the first effects of the home central bank's actions aimed at reducing fluctuations of the exchange rate, compared to a free float. The bank's actions may be then viewed as a *de facto* reduction of the target zone band over time, whilst the *de jure* band remains unchanged. Furthermore, t_{relax} can be interpreted as being the minimum time for agents to update their priors accurately, generating self-fulfilling expectations that create the honeymoon effect.

The inverse of the relaxation time is determined by the **spectral gap**, which is the distance between 0 and the smallest eigenvalue. We therefore have the relationship $(t_{\text{relax}})^{-1} = (\Omega_1^2 + \rho)$. The spectral gap controls the asymptotic time behavior of the expansion given by (10), and it is continuously dependent on risk β and band $\bar{f}$. This relationship is illustrated in Fig. 4.

Let us now study analytically the behavior of the solution Ω_1 of the transcendental Eq. (11). Writing $z = \sqrt{2}\Omega_1\bar{f}$, Eq. (11) implies that the product $\beta\bar{f}$ is the determinant of the amplitude of Ω_1. One can therefore immediately conclude that two limiting situations can be reached:

$$\begin{cases} \beta\bar{f} \ll 1 \quad \Rightarrow \quad z \lesssim \frac{\pi}{2} \quad \Rightarrow \quad \Omega_1 \lesssim \frac{\pi}{2\bar{f}} \quad \Rightarrow \quad t_{\text{relax}}^{-1} \lesssim \left[\frac{\pi}{2\bar{f}}\right]^2 + \frac{\beta^2}{2} + \alpha, \\ \beta\bar{f} \gg 1 \quad \Rightarrow \quad z \gtrsim \pi \quad \Rightarrow \quad \Omega_1 \gtrsim \frac{\pi}{\bar{f}} \quad \Rightarrow \quad t_{\text{relax}}^{-1} \gtrsim \left[\frac{\pi}{\bar{f}}\right]^2 + \frac{\beta^2}{2} + \alpha. \end{cases}$$

and therefore:

$$\frac{1}{\left[\frac{\pi}{\bar{f}}\right]^2 + \frac{\beta^2}{2} + \alpha} \leq t_{\text{relax}} \leq \frac{1}{\left[\frac{\pi}{2\bar{f}}\right]^2 + \frac{\beta^2}{2} + \alpha}. \tag{12}$$

Eq. (12), together with Fig. 4, shows how an increase in risk β affects t_{relax} more strongly when the exchange rate is allowed to float in a wider bandwidth $\bar{f}$.

4.2. Regime shifts and honeymoon effects

An unique phenomenon that arises in our framework, is the emergence of a *regime shift*. Fig. 5(b) shows that for a wide enough target band, beyond a threshold level of β, the relaxation time suddenly jumps to a much lower value and remains almost constant (though very slowly increasing) for further increases in risk. This happens because when the tendency β of the noise source driving the fundamental reaches and surpasses a certain level, the destabilizing risk component in the noise source overcomes the

[5] See Figure 2 in Crespo-Cuaresma et al. (2005).

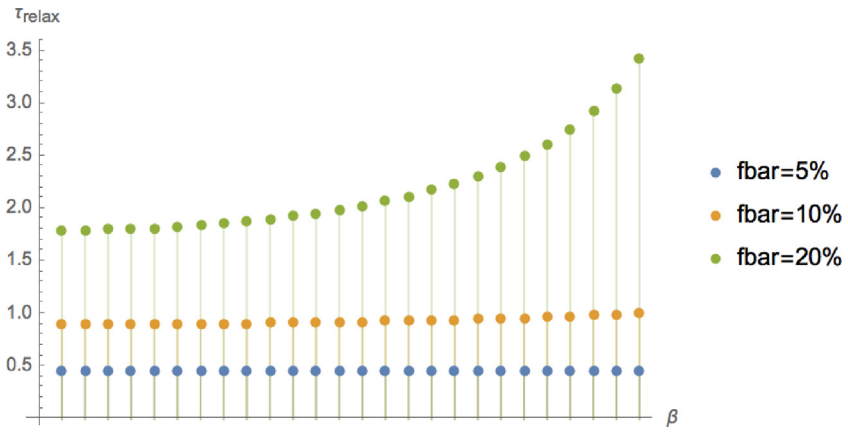

Fig. 4. Interaction between β and $\bar{f}$. This figure shows the interaction of varying risk (β) and varying the band size ($\bar{f}$). An increase in risk, for a given $\bar{f}$, implies that the lowest eigenvalue Ω_1 falls. The inverse of this value controls the t_{relax}.

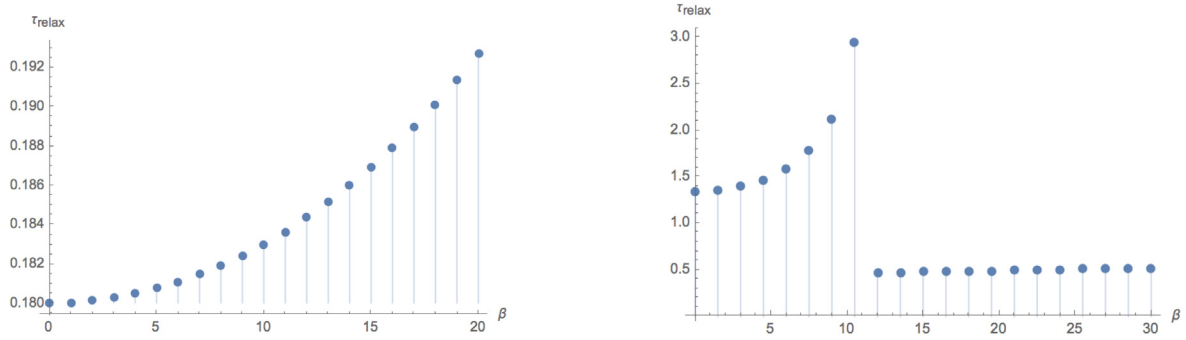

(a) $\bar{f} = 2\%$ (b) $\bar{f} = 15\%$

Fig. 5. Regime shift and eigenvalue jump as a function of risk, for different target bands.

diffusion. The force $\beta\mathcal{B}$ in the mean-preserving spread becomes the main driver of the stochastic process driving the fundamental, and therefore f_t becomes a process with a tendency to escape from its mean that is stronger than the tendency to diffuse around its central value. While this may look like a sudden emergence of supercredibility, it is in fact the opposite: the target zone cannot be feasibly maintained, as the fundamental process escapes its initial position with such force that it hits the band at every dt, and interventions need to be almost continuous. The central bank will have to either increase the size of the band or allow the spot rate to float freely. This has a direct implication for honeymoon effects, as shown in the following Proposition:

Proposition 2 (*Risk, Regime Shifts and Honeymoon Effects.*)**.** *There exists a threshold level of risk $\beta^e \in \mathbb{R}^+$ which generates a regime shift. This is caused by a jump in the spectrum Ω, as the elasticity with respect to the fundamental process of each eigenfunction ψ_k associated to the eigenvalue Ω_k must always match the underlying mean-preserving probability spread:*

$$\frac{\partial_f \psi_k(\Omega_k, f_t)}{\psi_k(\Omega_k, f_t)} = MPS(\beta, f_t) \qquad \forall\ \Omega_k(\beta, \bar{f}) \in \Omega. \tag{13}$$

For $\beta \geq \beta^e$, the smooth-fitting procedure at the boundaries cannot be applied and honeymoon effects when the fundamental approaches the band become unobtainable.

Proof. See Appendix C.

Proposition 2 implies that a high level of risk denies a central bank monetary autonomy up until the moment of entering the currency zone. This phenomenon is illustrated in Fig. 7. The first term in (13) is a total sensitivity term, closely related to the elasticity of the eigenfunction with respect to the fundamental, and it represents the overall variation of the exchange rate with the fundamental. The second term represents the increase in risk, as well as the destabilizing component that represents the tendency of the fundamental to hit the target bands. The solution of this equation yields the spectrum $\{\Omega_k\}$, for $k = \mathbb{N}^+$. The difference of the two terms represents the residual tendency of the home country fundamental to avoid converging to the target fundamental. The spectral gap, therefore, represents the intensity of the probability spread.

The regime shift will happen at a threshold value β^e, which can only be determined numerically, for which the spectral gap will suddenly jump upwards: the destabilizing force dominates the diffusive part and the first eigenvalue jumps higher. The oscillating part of the expansion increases in frequency, and the time-dependent exponential decay increases in speed. A graphical illustration is shown in Fig. 6: one can easily show that the lower bound for the threshold β^e is given by $1/\bar{f}$. This allows one to uncover the close relationship between the regime shift and the size of the target band. This regime shift **cannot** occur with a Gaussian process or with mean-reverting dynamics.

In the diffusion-driven regime (characterized by a relatively low $\beta < 1/\bar{f}$), one observes that an increase of risk implies a decrease in sensitivity, since t_{relax} is increasing. This may seem counterintuitive: but it must be remembered that at time $t = 0$, the initial condition is the stationary solution of the central bank-controlled diffusion for the given risk. Increasing β, therefore, is likely to load the stationary probability mass accumulated in the

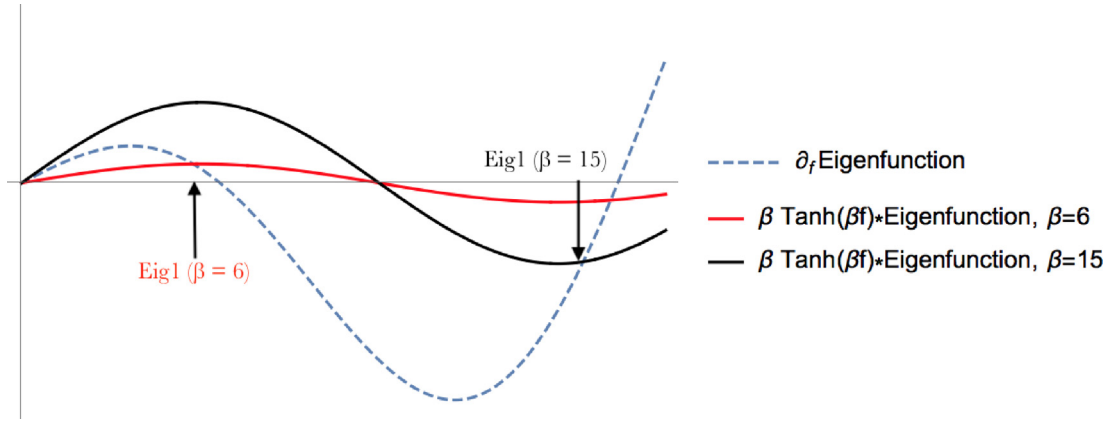

Fig. 6. Risk and eigenvalue jump. For $\beta = 15$ the regime shift has occurred: the force $\beta \tanh(\beta f)$ (black curve) overcomes the diffusion component and generates the first eigenvalue jump. For $\beta = 6$ (red curve), the regime has not yet shifted. Here $\bar{f} = 0.1$, $\sigma = 1, \alpha = 0.8$.

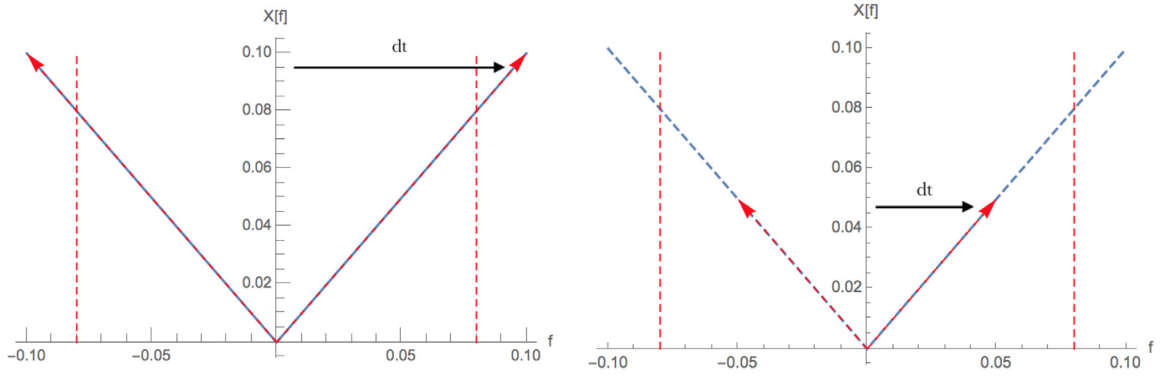

(a) $\beta > \beta^e$. No honeymoon effects (b) $\beta < \beta^e$.

Fig. 7. Risk threshold, distance to the bands and honeymoon effects: large risk shocks vs. diffusion-driven regimes.

vicinity of the target zone boundaries. Escape from this stationary state by bank action becomes more difficult, ultimately leading to an increase of t_{relax}. Conversely, in high risk regimes where $\beta > 1/\bar{f}$ and where the destabilizing dynamics dominate, the boundaries of the target zone are systematically hit by the fundamental. In this situation, the central bank will intervene almost entirely intramarginally regardless of whether the fundamental is actually close to the bands, since honeymoon effects cannot exist anymore. This result allows in Eq. (12) for a sudden reduction of the probability mass located at the bounds, and generates the sharp drop of t_{relax}. In other words, the shape of the target zone cannot be "heard" anymore, even if the spectrum is fully known: honeymoon effects vanish and the central bank operates in an infinitesimally narrow band.

This result provides new insight into target zone feasibility: if risk is too high, exchange rate expectations are no longer anchored to the band and the effectiveness of central bank intervention is greatly reduced. What the central bank could do is therefore either (i) to reduce risk, which in practice is often infeasible, or (ii) to increase the size of the target zone which itself is bounded by the free-float exchange rate volatility. The new size of the band would have to be large enough for the shape of this new target zone to be heard.

We can therefore also connect the threshold β_e at which the regime shift occurs to complete factor market integration: for lower levels of β, the home fundamental exhibits an idiosyncratic component anchored to its original dynamics that is stronger than its tendency to converge to the target fundamental. Once this component is overcome, the target zone ceases to exist and the currency starts floating. This may also help explain why countries with a high level of capital integration with the target currency may have higher costs in maintaining a target zone. This is precisely what Lera and Sornette (2015) illustrate with the case of the Swiss Franc floor between 2011–2015. In this particular case, the sustained pressure stemmed from the Swiss Franc being used as a safe asset in the middle of the European crisis.

4.3. Numerical simulations

The last contribution of our model lies in its generality, and how it can replicate all the exchange rate densities presented by the established target zone literature. We simulate central bank intervention by means of a symmetrized Euler scheme for stochastic differential equations. Since the original problem is a one-dimensional Neumann problem on the boundary $\partial D = [-\bar{f}, \bar{f}]$, the regulated SDE can be written as:

$$f_t = f_0 + \beta \int_0^t \tanh(\beta f_s) ds + \sigma \int_0^t dW_s + \int_0^t \gamma(f_s) ds,$$

where the hyperbolic tangent is the nonlinear drift stemming from external risk[6] and $\gamma(.)$ is the oblique reflection of the process on the boundary ∂D. This is the equivalent of the interventions, and we assume that for the unit vector field γ there exists a constant c so that $\gamma(x) \cdot \vec{n}(x) \geq c$ for all points x on

[6] This is an equivalent representation of (3): see Arcand et al. (2020) for further details.

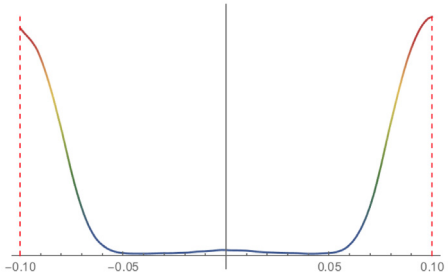

(a) Marginal intervention, LAW

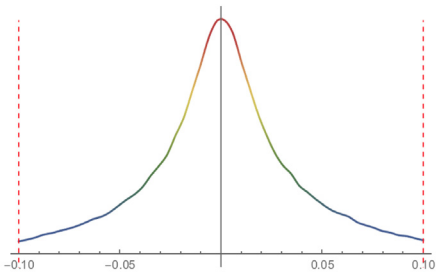

(b) Intramarginal intervention, pure reflection

Fig. 8. Exchange rate densities, $\beta = 0$.

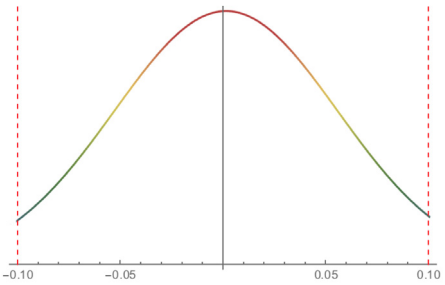

(a) Intramarginal intervention, LAW

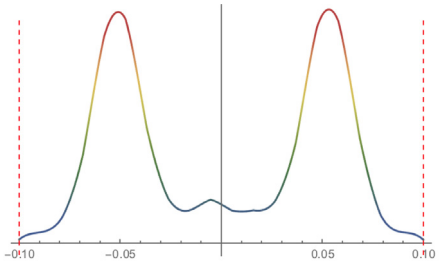

(b) Two-regime intervention, pure reflection

Fig. 9. Exchange rate densities, $\beta > 0, \beta < \beta^e$.

the boundary D. This can be interpreted as assuming bounded interventions. We use a regular mesh $[0, T]$ for the numerical simulation, for which the weak error is of order 0.5 when the reflection is normal (i.e. $\gamma = \vec{n}$), which is our case. We choose this method in order to obtain consistent Monte Carlo simulation of the resulting densities. The algorithm starts with $f_0 = 0$ and for any time t_i for which $f_{t_i} \in D$ we have for $t \in \Delta t = t_{i+1} - t_i$ that:

$$F_t^{N,i} = f_{t_i}^N + \hat{b}(f_{t_i}^N)(t - t_i) + \sigma(W_t - W_{t_i}),$$

as in the standard Euler–Maruyama scheme, and the nonlinear drift is approximated with a second-order stochastic Runge–Kutta method. If $F_{t+1}^{N,i} \notin \partial D$, then we set:

$$f_{t+1}^N = \pi_{\partial D}^{\gamma}(F_{t+1}^{N,i}) - \gamma(F_{t+1}^{N,i}),$$

where $\pi_{\partial D}(x)$ is the projection of x on the boundary ∂D parallel to the intervention γ. If $F_{t+1}^{N,i} \in \partial D$, then obviously $f_{t+1}^N = F_{t+1}^{N,i}$. For more references, see Bossy et al. (2004). The exchange rate path is then obtained by setting $X_t^N = X^*(f_t^N, T - t)$ for every $t \in [0, T]$. It is of fundamental importance to set Δt equal to the update ratio given by $1/\alpha$ in our model, so that the increment of the simulated exchange rate path has the same updating time frequency as the central bank.

We can now discuss two kinds of interventions: the kind that intervenes by reflecting the process so that it just stays within the band, sometimes called "leaning against the wind" (LAW), and the pure reflection variety, which projects the fundamental process by an amount equivalent to how much the process would have surpassed the boundary. This distinction can also be understood as being associated with the magnitude of reserves that the central bank has at its disposal in order to stabilize the fundamental process: the greater this quantity, the more likely it is that the intervention will be of the pure reflection type. We also assume that an intervention is effective instantaneously. As shown in Fig. 7, given our characterization of risk, the greater the β, the earlier the central bank will have to intervene, given the fundamental's increased tendency to escape towards the bands.

We present five possible scenarios by estimating Monte Carlo densities of the simulated exchange rate process: the first two correspond to the Gaussian case, where $\beta = 0$ with each of the two intervention strategies. The densities are obtained by Monte Carlo simulation of N sample paths, binning the data and limiting the bin size to zero to obtain the convolution density, then averaging over the N realizations and interpolating the resulting points. For more references on the method, see Asmussen and Glynn (2007). For all figures N is set to 5000, $\sigma = 0.1, r = 0.5, \alpha = 200, T = 3$ and the exchange rate target band to $\pm 10\%$. We obtain a realization path for each of the two and obtain both U-shaped (corresponding to the standard Krugman model) and hump-shaped densities, corresponding to the Dumas and Delgado (1992) framework. The realized densities are plotted in Fig. 8. We then simulate the case in which $\beta > 0$ but is not large enough to trigger the regime shift, each one with a different intervention strategy: in the marginal intervention case we obtain the two-regime density ($\beta = 5$) where *de facto* bands start to appear, as in the Bessec (2003) framework. For the intramarginal one we obtain a typical hump-shaped distribution. These results are shown in Fig. 9.

Finally, we present the case in which β is large enough ($\beta = 50$) to trigger the regime shift, and the band in fact ceases to exist: the tendency to escape leads to the fundamental process constantly surpassing the boundary, honeymoon effects are impossible and pure reflection intervention concentrates most of the realizations around the initial level. The target zone is untenable and the central bank must either increase the bandwidth or drop

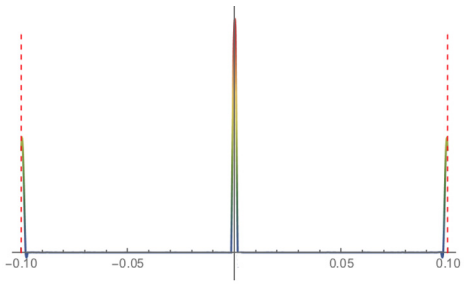

Target band too narrow given the level of underlying risk.

Fig. 10. Exchange rate densities, $\beta > \beta^e$.

the target zone altogether. For large N the exchange rate density becomes a Dirac delta function around the initial value of the fundamental, displayed in Fig. 10.

5. Policy implications and relevance

Our framework yields multiple interlinked policy implications.

First, we are able to characterize the *feasible band* in a target zone which allows central banks to enjoy honeymoon effects, reducing the cost of intervention for achieving the set parity. From (13) and the subsequent discussion one can obtain the *minimum* size $|\bar{f}| > 1/\beta$, which is directly related to the risk threshold that makes the target zone untenable. A central bank entering a target zone mechanism with a terminal exit time to another currency wants to limit the volatility of its exchange rate X_t versus the anchor currency below the free-float level of the anchor currency. This provides us with a natural condition for the *maximum* size of the band that the central bank can set as $|\bar{f}| \leq \sigma_z$, where σ_z is the long-term variance of the anchor currency. Considering the case of a target zone mechanism like ERM-II which has a band size of $\pm 15\%$, the above condition implies that it is unlikely that the ERM-II bands will be breached. The Euro has a long-run volatility versus most currencies that is lower than the ERM-II target band. If there were *no exposure* to external risk, it would be pointless to maintain a target zone with bands larger than σ_z.

The second policy contribution lies in establishing the *minimum time* that a target zone must be maintained before any successful convergence can be achieved, via the concept of characteristic relaxation time t_{relax}, directly connected to the spectral gap (12). The relaxation time determines the minimum time a target zone must be maintained in order to "feel" the first effects of the home country central bank's actions. The implications of this quantity for central bank policies are substantial: choosing an exit time below t_{relax} would imply setting up an unfeasible target zone, as t_{relax} controls the minimum time necessary for agents to update their previously held exchange rate expectations, generating self-fulfilling expectations that create the honeymoon effect.

A further implication of this mechanism is that a central bank cannot adopt a target currency overnight with an arbitrary parity being the close of day value of the target exchange rate. In such a case, agents would not have had time to update their expectations and this would force the central bank to use a larger proportion of its assets (in the target currency) defending the parity level. This opens up many different avenues of enquiry into the expectation generation process of agents in foreign exchange markets. If t_{relax} is the minimum time for agents to update their previously held exchange rate expectations, this means that higher degrees of agent risk aversion (higher β) will increase t_{relax}, which is an implication of our model. As shown by Osler (1995) and Lin (2008), this effect would work through the feasibility of the target zone in time shifting speculators' horizons towards short term speculation, where $t_{speculation} \leq t_{relax}$. This is a natural outcome of honeymoon effects, which make intervention cheaper for central banks and harder for speculators *after* t_{relax}. We find that t_{relax} is increasing with the magnitude of the risk aversion shifts, for $\beta \leq \beta_e$.

Our model does not deal with optimal choices: indeed, the only choice variable potentially available to the authorities is the time horizon T by which the required parity needs to obtain. If one chooses an exit time which is lower than the required minimum time at which parity can be reached (the relaxation time), the target zone exit time is not feasible. However, setting a T which is too high exposes one to increased business cycle risks, the dampening of which were a likely reason for entering a target zone in the first place.

5.1. Relevance

Our measure of fundamental risk can be used to fit a broad spectrum of global shocks which can destabilize exchange rate fundamentals. In Appendix E we show how inflation expectations (key fundamentals in the determination of exchange rates) of ERM-II countries follow a highly non-Gaussian distribution, compatible with our fundamental dynamics (4), and we provide alternative reduced-form interpretations of β as a source of destabilizing risk.

Our framework is also similar to the currency crisis models that study speculative attacks on managed exchange rate arrangements, which include target zones. These models maintain a Gaussian fundamental process but add state-dependent target zone commitment to incorporate endogenous devaluation risk (Flood and Marion, 1999; Obstfeld, 1996). With our measure of non-Gaussian external risk we achieve similar outcomes and can therefore study the feasibility of a target zone from a more general perspective, without assuming *any* central bank or government reaction function. Furthermore, the aforementioned models cannot explain how honeymoon effects can vanish under crises, a mechanism that can be captured only using our rigorous characterization of risk.

Our framework has substantial implications for managed exchange rate arrangements beyond target zones. It sheds light on the nature of external risk and points towards different strategies that central banks can adopt in order to limit negative spillovers from the global financial cycle. Negative spillovers that lead to capital flow reversals may induce exchange rate revaluations that are not in line with fundamentals, leading to increases in risk in (4) that could challenge the feasibility of the target zone. The optimal policy response in such a situation is to increase the risk-sharing between the home currency and the target currency central banks, which would reduce the pressure on the fundamental and return the risk β to a safe distance from the threshold β_e. This strategy may take the form of swap lines or joint intervention in times of large exchange market pressure.

Should such cooperation not be possible, home central banks may have to use the second-best option of macro-prudential and capital flow measures limiting capital flow volatility from translating to exchange rate volatility. Dorrucci et al. (2020) show that the European Central Bank (ECB) has made progress towards the second-best policy outcome by mandating that countries joining the Euro through the ERM-II have to join the European banking union and be subject to enhanced banking sector supervision.[7]

[7] The majority of the capital flow volatility realized by ERM-II countries in the 2000's was via banking sector capital flows rather than portfolio flows.

The use of swap-lines by the ECB for ERM-II countries during the COVID-19 pandemic is an example of pro-active policy ensuring the feasibility of target zones. While provision of emergency swap lines is not standard practice, given legitimate concerns of moral hazard for new member states, our model shows how it may be useful in allowing for a successful convergence.

The policy relevance of our framework for finite-time target zones is further illustrated outside of Europe by the attempts by the Economic Community of West African States' (ECOWAS) to get 15 countries in West Africa to adopt a common currency (the ECO). ECOWAS had an ambitious and common target zone time horizon of one year for all 15 participating countries to transition to the ECO from the West African CFA Franc prior to the onset of the COVID-19 pandemic. The original plan for Eco adoption did not factor in the inherent idiosyncratic risk faced by individual West African central banks and ignored external risk factors. This translates directly to our framework, where the risk β may generate a relaxation time t_{relax} for individual states that may be larger than the proposed convergence time T. In light of the COVID-19 pandemic and its heterogeneous impact on the ECOWAS member states, the final time for convergence has been moved from 2021 to 2027, yielding a more realistic time frame for adoption of the Eco. Our framework can guide the participating central banks away from unrealistic time horizons with potentially long lasting consequences for both their own credibility and for the overall likelihood of creating the new common currency.

5.2. Extensions

Lastly, in the Appendices we provide a set of extensions to our framework. In this paper we choose to focus on a fundamental process that remains stationary in distribution around its long-run level, here normalized to 0 without loss of generality. This is the case for most target zones. However, if the fundamental was substantially misaligned from its long-run level, then the choice of a mean-reverting process could be more appropriate. The analysis of this case is presented in Appendices F and G, where we fully solve both Ornstein–Uhlenbeck (O–U) and non-Gaussian, softly attractive dynamics. The latter can be of interest for researchers as an alternative to the O–U process, since it allows one to again escape Gaussianity and to model an ergodic process with light attraction towards its long-run level, whilst maintaining analytical tractability.

6. Conclusions

Can one hear the shape of a target zone? The answer depends on whether the target zone is set up in a feasible way given the underlying fundamental risk that counteracts central bank efforts. In this paper we have explored the implications of extending exchange rate target zone modeling to non-stationary dynamics and heavy, non-Gaussian tails stemming from time-varying investor risk aversion, which lead to mean-preserving risk increases in the fundamental distribution. Our framework leads to a natural interpretation of target zone feasibility, driven by the interplay between two contrasting forces: a destabilizing effect driven by risk which pushes the exchange rate towards the bands, and a stabilizing diffusive force. For a given band, there is a maximum level of risk that allows one to "hear" the target zone. We show how our model effectively endogenizes the presence of the bands by the exchange rate expectations, and how the interplay between risk and target band has key implications for the credibility of the zone itself, as well as the possibility of honeymoon effects. Intervention is shown to be both marginal and intramarginal, depending on how much the central bank feels both the distance to the target zone band and the presence of external risk. The potential emergence of regime shifts, moreover, can further erode target zone credibility. This allows the methods employed in this paper to be applied to a wide range of situations. A relevant future extension of our work would be its empirical counterpart, consisting in the structural estimation of the model parameters and an explicit computation of the relaxation time, thus effectively providing the feasible band size as well as a lower bound for the necessary time for a central bank to reach the desired parity for its currency.

Declaration of competing interest

By means of this document the authors declare that they have no competing interests whatsoever.

Data availability

Data will be made available on request.

Appendix A. Monetary model of exchange rate determination

Let us start with a standard flexible-price monetary model of exchange rate as in Ajevskis (2011). The money demand function is given as

$$m_t - p_t = \theta^y y_t - \theta i_t + \epsilon \tag{14}$$

where m is log of the domestic money supply, p is log of the domestic price level, y is the log of domestic output and i is the nominal interest rate. θ_y is the semi-elasticity of money demand with respect to output whereas θ_i is the absolute value of the semi-elasticity of money demand with respect to the domestic nominal interest rate and ϵ is a money demand shock. The second block is given by the expression for the real exchange rate q which is defined as

$$q_t = X_t + p_t^* - p_t$$

where p^* is the log of the foreign price level. The third block of this model is the uncovered interest rate parity condition which in a linearized form is given by

$$\mathbb{E}dX_t = (i_t - i_t^*) - \eta_t \tag{15}$$

where $\mathbb{E}dX_t$ is the expectation of the exchange rate conditional on information available until time t and i_t^* is the foreign interest rate. η_t is a time-varying risk premium and is a consequence of risk-averse foreign investors who demand a higher compensation for holding home bonds and depends on investors' risk aversion. Let us consider that investors face a standard problem of consumption of two bonds, home and foreign, with concave utility $U(c_t)$ discounted at γ. B_t^h is the holding of home (small open economy) bonds, B_t^f is the holding of foreign bonds by a representative agent. Consumption and bond holdings in period t and $t+1$ are given by the problem

$$\begin{aligned} \max_{c_{t+1}, B_t^h, B_t^f} \quad & \sum_{t=0}^{\infty} \gamma^t U(c_t) \\ c_t &= B_t^h + X_t B_t^f \\ \mathbb{E}[c_{t+1}] &= (1+i_t)B_t^h + \mathbb{E}[X_{t+1}](1+i_t^*)B_t^f. \end{aligned}$$

Solving this problem leads straightforwardly to Eq. (1). Using Eqs. (14), (15) and (1), we recover the monetary model of the exchange rate as given by

$$\theta \mathbb{E}dX_t \underbrace{\underbrace{-\theta^y y_t + q_t + p_t^* + \theta i_t^* - \epsilon}_{v_t} + \theta\eta_t + m_t}_{f_t} = X_t \tag{3}$$

$$X_t = \theta \mathbb{E}_t\{dX_t\} + v_t + \theta\eta_t + m_t$$
$$= \theta\left(\mathbb{E}_t\{dX_t\} + \frac{d\mathbb{Q}}{d\tilde{\mathbb{Q}}}\right) + v_t + m_t. \quad (16)$$

In the literature the velocity v_t is usually modeled as a Brownian motion. In order to include η_t, the time-varying risk premium, we modify the Brownian motion to include the incremental risk generated by varying investor risk aversion by means of (2). Intervention happens at the boundaries $\underline{f}, \bar{f}$, at which the central bank undergoes infinitesimal adjustments of money supply m_t in order to keep the fundamental in the band. Eqs. (3), (5) and the boundary conditions then follow directly.

Appendix B. Proof of Proposition 1

Using Itô calculus, Eq. (5) can be written as follows:

$$\partial_t X(t,f) + \frac{\sigma^2}{2}\partial_{ff}X(t,f) + \beta\mathcal{B}\partial_f X(t,f) - \alpha X(t,f) = -\alpha f. \quad (17)$$

Note the presence of the additional term $\partial_t X(f)$ in Eq. (23) which does not appear when one focuses only on stationary situations. As shown in Arcand et al. (2020), Eq. (23) can be written equivalently as the nonlinear partial differential equation given by

$$\partial_t X(t,f) + \frac{1}{2}\partial_{ff}X(t,f) + \beta\tanh(\beta f)\partial_f X(t,f) - \alpha X(t,f) = -\alpha f. \quad (18)$$

Using the superposition principle, the solution of (18) can be written as the sum of the time-independent stationary solution and the non-stationary solution:

$$X(\tau,f) = X^*(\tau,f) + X_S(f). \quad (19)$$

For the derivation of the stationary solution, we first introduce the following *Ansatz*:

$$\partial_f X(t,f) = Y(t,f)/\cosh(\beta f). \quad (20)$$

This leads to the following transformations:

$$X = \frac{Y}{\cosh(\beta f)},$$
$$\beta\tanh(\beta f)\partial_f X = \left[\beta\frac{\sinh(\beta f)}{\cosh(\beta f)}\right]\left[-\beta\frac{\sinh(\beta f)}{\cosh^2(\beta f)} + \frac{\partial_f Y}{\cosh(\beta f)}\right]$$
$$= -\beta^2\frac{\sinh^2(\beta f)}{\cosh^3(\beta f)}Y + \beta\partial_f Y\frac{\sinh(\beta f)}{\cosh^2(\beta f)},$$
$$\frac{1}{2}\partial_{ff}X = \frac{1}{2\cosh(\beta f)}\partial_{ff}Y - \frac{\beta\sinh(\beta f)}{\cosh^2(\beta f)}\partial_f Y$$
$$-\frac{\beta^2}{2}\frac{Y}{\cosh(\beta f)} + \beta^2\frac{\sinh^2(\beta f)}{\cosh^3(\beta f)}Y,$$

which substituted in (18) yield the following linearization:

$$\partial_t Y(t,f) + \frac{1}{2}\partial_{ff}Y(t,f) - \left[\frac{\beta^2}{2} + \alpha\right]Y(t,f) = -\alpha f\cosh(\beta f). \quad (21)$$

Setting $\partial_t = 0$ one obtains a nonlinear ODE in f which has the closed form solution as given by

$$\begin{cases} \mathcal{Y}_1(f) = \exp\left\{+\sqrt{\left[\beta^2 + 2\alpha\right]}f\right\}, \\ \mathcal{Y}_2(f) = \exp\left\{-\sqrt{\left[\beta^2 + 2\alpha\right]}f\right\}, \\ Y_P(f) = \frac{2\alpha(f(2\alpha)\cosh(\beta f) + 2\beta\sinh(\beta f))}{(2\alpha)^2} \end{cases} \quad (22)$$

which is the sum of the general solution (two opposite-sided exponentials) and a particular solution. Obtaining the general solution is a simple exercise and thus omitted, while the particular solution requires a little more attention. We introduce another *Ansatz*:

$$\begin{cases} Y = [Rf\cosh(\beta f) + S\sinh(\beta f)], \\ \partial_f Y = [R\cosh(\beta f) + Rf\beta\sinh(\beta f) + S\beta\cosh(\beta f)], \\ \partial_{ff}Y = \left[2R\beta\sinh(\beta f) + Rf\beta^2\cosh(\beta f) + S\beta^2\sinh(\beta f)\right. \end{cases}$$

We therefore have:

$$\tfrac{1}{2}\partial_{ff}Y - \left[\alpha + \tfrac{1}{2}\beta^2\right]Y + \alpha f\cosh(\beta f) =$$
$$\left[\tfrac{1}{2}R\beta^2 - \left[\alpha + \tfrac{1}{2}\beta^2\right]R + \alpha\right]f\cosh(\beta f) + \left[R\beta + \tfrac{1}{2}S\beta^2\right.$$
$$\left. - \left[\alpha + \tfrac{1}{2}\beta^2\right]S\right]\sinh(\beta f) = 0.$$

Matching coefficients we obtain:

$$\begin{cases} \left[\tfrac{1}{2}R\beta^2 - (\alpha + \tfrac{1}{2}\beta^2)R + \alpha\right] = 0, \\ \left[R\beta + \tfrac{1}{2}S\beta^2 - \left[\alpha + \tfrac{1}{2}\beta^2\right]S\right] = 0. \end{cases}$$

which implies $R = 1, S = \frac{\beta}{\alpha}$ and thus

$$Y_P = \frac{\alpha f\cosh(\beta f) + \beta\sinh(\beta f)}{\alpha}.$$

Inverting the transformation back to X one obtains (8). In Eqs. (8) the pair of constants A and B can be determined by smooth fitting at the bounds $\underline{f} = -\bar{f}$:

$$\partial_f X_S(f)\,|_{f=\underline{f}} = \partial_f X_S(f)\,|_{f=\bar{f}} = 0.$$

The two constants of integration A and B can be obtained in closed form but their expression is lengthy and is therefore omitted.

We now turn to the non-stationary dynamics. At a given time horizon $t = T$, we fix the predetermined non-stationary part of the exchange rate at exit time $X(T,f) = 0$. In terms of the backward time $\tau = T - t$, we write the transformation $X^*(\tau,f) = Y^*(\tau,f)/\cosh(\beta f)$. We then need to solve the following nonlinear boundary value problem:

$$\begin{cases} \partial_\tau X(\tau,f) - \frac{1}{2}\partial_{ff}X(\tau,f) - \beta\tanh(\beta f)\partial_f X(\tau,f) + \alpha X(\tau,f) \\ \quad = +\alpha f, \\ X(0,f) = 0 \\ \partial_f X^*(\tau,f)\,|_{f=\underline{f}} = 0 \\ \partial_f X^*(\tau,f)\,|_{f=\bar{f}} = 0 \end{cases} \quad (23)$$

Writing $X(\tau,f) = X^*(\tau,f) + X_S(f)$, Eq. (23) implies:

$$-\frac{1}{2}\partial_{ff}X_S(f) - \beta\tanh(\beta f)\partial_f X_S(f) + \alpha X_S(f) = \alpha f, \quad (24)$$
$$\partial_\tau X^*(\tau,f) - \frac{1}{2}\partial_{ff}X(\tau,f) - \beta\tanh(\beta f)\partial_f X(\tau,(f)) + \alpha X^*(\tau,f) = 0$$

While the first line in Eq. (24) has already being solved, the second line needs now to be discussed. Writing again $X^*(\tau,f)\cosh(\beta f) := Y^*(\tau,f)$, we obtain:

$$\partial_\tau Y^*(\tau,f) - \frac{1}{2}\partial_{ff}Y^*(\tau,f) + \left[\frac{\beta^2}{2} + \alpha\right]Y^*(\tau,f) = 0. \quad (25)$$

The boundary conditions given by Eq. (9) impose:

$$\begin{cases} \partial_f X^*(\tau,f)\,|_{f=\underline{f}} = 0 \quad \Rightarrow \quad \left\{\left[\partial_f Y^*(\tau,f)\right] - \beta\tanh(\beta f)Y^*(\tau,f)\right\}\,|_{f=\underline{f}} = 0, \\ \partial_f X^*(\tau,f)\,|_{f=\bar{f}} = 0 \quad \Rightarrow \quad \left\{\left[\partial_f Y^*(\tau,f)\right] - \beta\tanh(\beta f)Y^*(\tau,f)\right\}\,|_{f=\bar{f}} = 0. \end{cases} \quad (26)$$

We express the solution $Y(\tau, f)$ as $Y^*(\tau, f) = \phi(\tau)\psi(f)$, and proceed to solve this equation by separation of variables and expansion over the basis of a complete set of orthogonal eigenfunctions. The solution can be expressed as $Y^*(\tau, f) = \phi(\tau)\psi(f)$, and therefore we can write it as

$$\frac{\dot{\phi}(\tau)}{\phi(\tau)} = \lambda_k = \frac{1}{2}\frac{\psi''(f)}{\psi(f)} - \rho$$

where $\rho = \left[\frac{\beta^2}{2} + \alpha\right]$.

The time-dependent part solves to $\psi(\tau) = \exp(\tau\lambda_k)$, and the fundamental-dependent part can be written as the ordinary differential equation

$$\psi''(f) - 2(\lambda_k + \rho)\psi(f) = \psi''(f) + 2\Omega_k^2\psi(f) = 0.$$

Solving for ψ one obtains the eigenfunctions

$$\psi_k(f) = c_1 \cos\left(\sqrt{2}\Omega_k f_t\right) + c_2 \sin\left(\sqrt{2}\Omega_k f_t\right).$$

Sturm–Liouville theory allows us to state that on the interval $[-\bar{f}, +\bar{f}]$, one has a complete set of orthogonal eigenfunctions $\psi_k(f)$ satisfying Eq. (9) which form an orthogonal basis for the $2\bar{f}$-well-behaving functions space. Smooth-fitting conditions impose $c_1 = 0, c_2 = 1$ and we obtain the form of the eigenfunctions

$$\psi_k(f) = \sin\left(\sqrt{2}\Omega_k f\right) \in [\underline{f}, \bar{f}], k = \mathbb{N}^+, \tag{27}$$

where each eigenvalue Ω_k solves the transcendental equation:

$$\sqrt{2}\Omega_k \cot\left(\sqrt{2}\Omega_k \bar{f}\right) = \beta \tanh(\beta\bar{f}). \tag{28}$$

as given by (27). By regularity of the Sturm–Liouville problem we know that the eigenvalues are real and span a discrete spectrum:

$$\{\Omega_k\} \coloneqq \left\{\Omega_k(\beta, \bar{f})\right\}, k \in \mathbb{N}^+.$$

and can therefore be ordered as:

$$\Omega_1(\beta, \bar{f}) < \Omega_2(\beta, \bar{f}) < \cdots \Omega_k(\beta, \bar{f}).$$

The Fourier coefficients follow in their standard form, using the stationary equation $X_S(f_t)$, and we finally obtain (10).

Appendix C. Proof of Proposition 2

We now briefly discuss the connection between risk and the honeymoon effect, and how such effects cannot be obtained when the destabilizing effects of risk shocks in the fundamental are too strong. For illustrative purposes, let us consider a baseline case of our model in a symmetric band $[-\bar{f}, \bar{f}]$ around the parity 0, and let us compare our model with the standard Gaussian one. Omitting time dependency, we have again the framework given by

$$X = f + \frac{1}{\alpha}\frac{\mathbb{E}\{dX\}}{dt},$$

which leads to the following pair of PDEs, depending on the form of the fundamental process.

$$\begin{cases} X = f + \frac{1}{2}\partial_{ff}[X(f)] & \text{(Gaussian)}, \\ X = f + \frac{1}{2}\partial_{ff}[X(f)] + \beta\tanh(\beta f)\partial_f[X(f)] & \text{(Ours)}. \end{cases}$$

We now focus on the stationary regime for which we obtain the general solutions:

$$\begin{cases} X(f) = f + A_0\sinh(\rho_0 f), & \text{(Gaussian)}, \\ X(f) = f + A_\beta\frac{\sinh(\rho_\beta f)}{\cosh(\beta f)}, & \text{(Ours)}, \end{cases}$$

where $\rho_\beta = \sqrt{\beta^2 + 4\alpha}$ and A_β is a yet undetermined amplitude. We now apply the smooth fitting procedure at the target level $+\bar{f}$.[8]

For the standard Gaussian framework we have $X(f) \mapsto X_0(f) = f + a\sinh(\rho_0 f)$, since $\beta = 0$ and consequently $\rho \mapsto \rho_0 \coloneqq \sqrt{\frac{2\alpha}{\sigma^2}}$. We therefore have :

$$X_0(f) = a\tanh(\rho_0 f) + f, \qquad \rho_0 = \sqrt{\frac{2\alpha}{\sigma^2}},$$

which is the same result as in the standard Gaussian model. In particular, denote $W \in \mathbb{R}$ the contact point with the target boundary $\pm\bar{f}$, we have

$$\begin{cases} \bar{f} = X_0(W) \quad \Rightarrow \quad F = W + a\tanh(\rho_0 W), \\ 0 = 1 + \rho_0 a\cosh(\rho_0 W) \end{cases} \tag{29}$$

because of the smooth-fitting boundary conditions on the first derivative. From the second line in Eq. (29), we conclude immediately that:

$$a = \frac{-1}{\rho_0\cosh(\rho_0 W)}.$$

and accordingly, we end with:

$$X_0(f) = f - \frac{\sinh(\rho_0 f)}{\rho_0\cosh(\rho_0 W)} \tag{30}$$

Furthermore, we can verify that $W \in \mathbb{R}^+$ for all values of the parameter $\rho_0 > 0$. Eq. (30) implies that:

$$W - F = \frac{\tanh(\rho_0 W)}{\rho_0}.$$

It can be immediately seen that the last equation always possesses a single solution $W \in \mathbb{R}^+$. Let us now examine the paper's main framework, the case where $\beta > 0$. In this case, for a target zone with band size F and a smooth contact point W, we have:

$$\begin{cases} F = W + a\frac{\sinh(\rho W)}{\cosh(\beta W)} + \omega\tanh(\beta W) \\ 0 = 1 + \frac{a}{\cosh(\beta W)}\left[\rho\cosh(\rho W) - \beta\sinh(\rho W)\tanh(\beta W)\right] \\ \quad + \frac{\omega\beta}{\cosh^2(\beta W)}. \end{cases} \tag{31}$$

The second line of the last equation implies:

$$a = -\frac{\cosh^2(\beta W) + \beta\omega}{\cosh(\beta W)\cosh(\rho W)\underbrace{\left[\rho\tanh(\rho W) - \beta\tanh(\beta W)\right]}_{\coloneqq\Delta}}.$$

From the last line, let us consider the equation $\Delta = 0$. First we remember from the very definition that $\rho \geq \beta$ and hence the equation:

$$\frac{\rho}{\beta}\tanh(\rho W) = \tan(\beta W) \qquad \Leftrightarrow \qquad \Delta = 0.$$

Since $\frac{\rho}{\beta} > 1$ the last equation necessarily admits a solution $\pm W_c$. Note in addition that for a pair of βs such that $\beta_1 < \beta_2$, we have:

$$\beta_1 > \beta_2 \quad \Leftrightarrow \qquad W_{c,1} < W_{c,2} \tag{32}$$

[8] Due to the symmetry, we have here only one amplitude$A$ to determine since only one boundary needs to be considered.

and for $\beta \to \infty$, we have $W_c \to 0$. Now from W solving the first line of Eq. (31), we may have the alternatives:

$$\begin{aligned} &(a) \quad W_c < W, \\ &(b) \quad W_c \geq W. \end{aligned} \tag{33}$$

Since the contact point W_c decreases as β increases, there exists a β^e for which $W_c = W$. For all $\beta > \beta_e$, standard boundary fitting techniques cannot be applied as in the Gaussian case, and hence the limit $W = W_c$ explains the regime shift observed in the spectrum. This is due to the fact that for large β the honeymoon effect range becomes effectively large enough to preclude the possible existence of a target zone. The eigenvalue jump can be obtained by examining the boundary conditions given by (26), and separating the contribution to the smooth-fitting at the boundaries given by the eigenfunction from the one given by the fundamental drift and obtain:

$$\frac{\partial_f \sin\left(\sqrt{2}\Omega_k f_t\right)}{\sin\left(\sqrt{2}\Omega_k f_t\right)} - \beta \tanh(\beta f_t) = 0.$$

By noticing that $\beta \tanh(\beta f)$ is equivalent to $\beta\mathcal{B}$, and is thus the mean-preserving spread caused by increases in fundamental risk, one obtains

$$\frac{\partial_f \psi_k(\Omega_k, f_t)}{\psi_k(\Omega_k, f_t)} - \mathrm{MPS}(\beta, f_t) = 0$$

and we obtain (13).

Appendix D. Noise sources driving the fundamental

Let us now assume that the fundamental is driven by a pair of noise sources, namely (i) composite shocks v_t and (ii) fluctuations in the money supply m_t, given by Gaussian noise around a drift μ. We therefore add another source of noise, but we are not necessarily increasing the risk in the fundamental process. We then have

$$\begin{cases} df_t = \sigma_1 dW_{1,t} + dm_t, \\ dm_t = \mu dt + \sigma_2 dW_{2,t}, \qquad m_{t=0} = m_0. \end{cases} \tag{34}$$

where the noise sources $dW_{1,t}$ and $dW_{2,t}$ are two independent White Gaussian Noise (WGN) processes. We then obtain f_t as a Gaussian process, since trivially

$$df_t = \mu dt + \sqrt{\sigma_1^2 + \sigma_2^2} dW_t$$

and we are exactly in the standard framework (in the literature it is usually the case that $\mu = 0$), only with a change in variance. If however we wish to incorporate a general increase in risk, and one that may represent the force that was discussed in Section 2, we can write the following more general framework:

$$\begin{cases} df_t = \sigma_1 dW_{1,t} + dm_t, \\ dz_{\beta,t} = \zeta(\beta; z_t)dt + \sigma_2(\beta) dW_{2,t}, \qquad z_{t=0} = 0. \end{cases}$$

where $\beta \geq 0$ is a control parameter and the repulsive drift $\zeta(\beta; z) = -\zeta(\beta; -z) < 0$ models an extra risk source via a dynamic zero mean process. We parametrize risk with β, and therefore $\beta = 0$ simply implies $\sigma_2(\beta) = \zeta(0; z_t) = 0$ implying that the process is Gaussian and driven entirely by the composite shock process. Our candidate for ζ is the DMPS process:

$$df_t = \sigma_1 dW_{1,t} + dz_t = \beta \tanh(\beta z_t)dt + \sigma_1 dW_{1,t} + \sigma_2(\beta) dW_{2,t}$$

$$\Downarrow$$

$$dz_t = \beta \tanh(\beta z_t)dt + \left[\sqrt{\sigma_1^2 + \sigma_2^2(\beta)}\right] dW_t, \quad z_{t=0} = 0.$$

where we used the fact that the difference between two independent WGN's is again a WGN with variance as given in the previous equation. Alternatively one may formally write:

$$df_t = \sigma_1 dW_{1,t} + \beta \tanh\left[\beta \overbrace{(f_t - \sigma_1 W_{1,t})}^{z_t}\right] dt + \sigma_2(\beta) dW_{2,t} =$$

$$\beta \tanh\left[\beta \overbrace{(f_t - \sigma_1 W_{1,t})}^{z_t}\right] dt + \left[\sqrt{\sigma_1^2 + \sigma_2^2(\beta)}\right] dW_t,$$

Using the initial Eq. (5) and the previous equation and applying Itô's lemma to the functional $X(f_t, t)$, we obtain:

$$\begin{aligned} \tfrac{1}{\alpha} \Bigg\{ &\partial_t X(f,t) + \partial_f X(f,t) \underbrace{\mathbb{E}\left\{\beta \tanh\left[\beta(f_t - \sigma_1 W_{1,t})\right]\right\}}_{=\beta \tanh[\beta(f)]} \\ &+ \left[\sigma_1^2 + \sigma_2^2(\beta)\right] \partial_{ff} X(f,t) \Bigg\} = X_t - f_t \end{aligned} \tag{35}$$

In Eq. (35), the under-brace equality follows since all odd moments in the expansion of the hyperbolic tangent vanish and the $\tanh(x)$ is itself an odd function. Now, normalizing so as to have $\left[\sigma_1^2 + \sigma_2^2(\beta)\right] = \sigma^2$, we are in the nominal setting of our paper.

Appendix E. Alternative interpretations of risk

Destabilization is intrinsically connected to risk in the fundamental process. Besides the structural interpretation of risk as stemming from time-varying investor risk aversion, one could think of a variety of other interpretations for the parameter λ of increasing risk, which generates mean-preserving spreads in the density of the exchange rate fundamentals. A quick glance at the left-hand panel of Fig. 11 shows that the difference in inflation expectations, one of the key fundamentals in the determination of exchange rate target zones, is undoubtedly non-Gaussian, exhibits substantially heavier tails and presents bimodal tendencies stemming from both inflationary and deflationary pressures shifting probability away from the center. Such risk dynamics cannot be represented by the variance of Gaussian fluctuations, as they cannot affect the distribution tails, but rather requires the presence of forces that increase the tendency of the fundamental process to escape its long-run level. The right-hand panel of Fig. 11 shows the transition density of the DMPS process at an arbitrary time for increasing risk, providing a better fit for the empirical densities.

Another way of interpreting the risk parameter of our framework could be via the presence of capital flows, especially in how the magnitude and the drivers of capital flows matter in determining the stabilization effects. First, capital flows may be driven by push factors creating cycles of bonanzas and sudden stops seen with New Member States. Hansson and Randveer (2013) argue that capital flow dynamics were the key driver for cyclical developments in the Baltic ERM economies. This might be an issue for a small target zone country if the capital flows

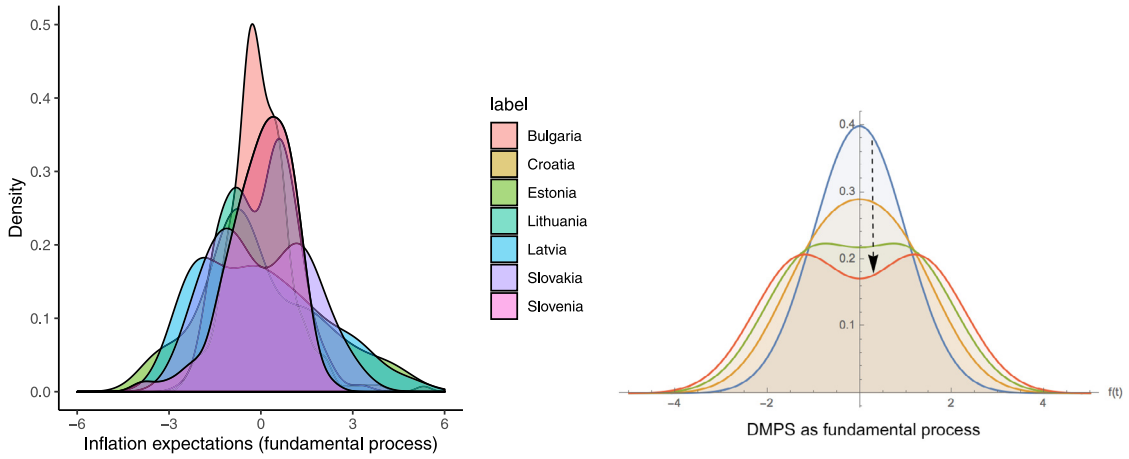

Fig. 11. Estimated densities of the fundamental process (inflation expectations) for ERM-II currencies. (Left panel) Centered difference between Euro area inflation expectations and target zone country inflation expectations, for the time each currency was in the target zone with the Euro. Kolmogorov–Smirnov tests greatly reject each hypothesis of Gaussianity. The data for inflation expectations comes from the Euro Commission's Joint Harmonized Consumer Survey. For more details we refer to Arioli et al. (2017). (Right panel) Transition densities of the fundamental process with mean-preserving spreads (DMPS) at time $t = 1$, each with risk increases in the direction of the arrow.

generate excess appreciation or depreciation pressure weakening the feasibility of the target zone. This is particularly problematic if there is a sudden stop with reallocation of capital flows to more productive economies in the target zone as seen during the Eurozone crisis (Ghosh et al., 2020). Furthermore, assuming the absence of macro-prudential tools, capital flow volatility may generate foreign exchange intervention volatility inside the target zone, as the use of interest rates as a monetary policy tool can generate further pro-cyclicality in capital flows. This nexus between capital flows and target zone management may destabilize the convergence in the inflation process of the target zone country. This is the key source of additional risk in our setting. Consider the real interest rate version of the UIP condition:

$$\mathbb{E}\{dX_t\} = (r_t - r_t^*)dt + \mathbb{E}\left\{d\pi_t - d\pi_t^*\right\},$$

where π^* is the target country's inflation measure and π is home inflation. If there are high capital inflows that need to be counteracted by (unsterilized) intervention, this would generate a lower real interest rate of financing by putting downward pressure on r_t. This additional supply of credit is likely to increase $\mathbb{E}\{d\pi_t\}$. This would require an interest rate response by the national central bank, in the absence of macro-prudential tools. We can see that in this particular case, increasing interest rates may be procyclical to capital flows as long as the inflation process responds positively to the interest rate hike, causing a loss of monetary autonomy if the process is self-reinforcing. A destabilizing outcome of this scenario would be if the inflation process does not respond to the interest rate moves and causes an outflow of capital. This would jeopardize the feasibility of the target zone and could cause the gap between r_t and r_t^* to become larger than before entering the target zone. The standard approach of modeling risk in the target zone does not consider the risk stemming from the currency union itself. If the target currency union has real interest rate changes through lower expected inflation surprises, it will also affect the stability of the target zone through the capital flow mechanism we have described.[9] Lastly, we note that our characterization of risk as destabilizations caused by capital flows can be further extended to any source of external risk, and our model framework would still apply.

Appendix F. Attracting drift: mean-reverting dynamics

A similar discussion can be developed for mean-reverting (Ornstein–Uhlenbeck) fundamental dynamics reflected inside an interval $[\underline{f}, \bar{f}]$. In this section, the fundamental is driven by the mean-reverting dynamics:

$$df = \lambda(\mu - f)dt + \sigma dW_t,$$

where μ is the "long-run" level of the fundamental, and λ is now the speed of convergence, to highlight the mean-reverting equivalent of the DMPS process. Following the previous exposition, we can obtain the full solution for the exchange rate $X^*(t, f)$ as the solution of

$$\partial_t X + \frac{\sigma^2}{2}\partial_{ff} X + \lambda(\mu - f)\partial_f X - \alpha X = -\alpha f.$$

As before, we have the stationary solution for a vanishing ∂_t, and here it reads

$$\begin{aligned} X_S(f) = {} & A\ {}_1F_1\left[\frac{\alpha}{2\lambda}, \frac{1}{2}; \frac{\lambda}{\sigma^2}(f-\mu)^2\right] \\ & + B\frac{\sqrt{\lambda}}{\sigma}(f-\mu)\ {}_1F_1\left[\frac{\alpha}{2\lambda} + \frac{1}{2}, \frac{3}{2}; \frac{\lambda}{\sigma^2}(f-\mu)^2\right] \\ & + \left[\frac{\lambda\mu f + \alpha}{\lambda + \alpha}\right] \end{aligned} \tag{36}$$

where ${}_1F_1[a, b; x]$ is the confluent hypergeometric function. The integration constants A and B, as before, are determined via smooth pasting at the target zone boundaries, namely: $\partial X_S(f)|_{f=\underline{f}} = \partial X_S(f)|_{f=\bar{f}} = 0$. Note that if $\mu = 0$, then $A = 0$. Fig. 12 shows the stationary dynamics of the exchange rate as a function of the fundamental, for different values of the long-run level μ and noise variance σ. The band is assumed symmetric around 0, and $\bar{f} = 10\%$.

The associated Sturm–Liouville equation is now given by

$$\frac{\sigma^2}{2}\partial_{ff} X + \lambda(\mu - f)\partial_f X + \alpha X = 0,$$

and the spectrum of the process can be obtained explicitly by solving a transcendental equation involving Weber parabolic

[9] For simplicity, we do not consider the currency union having positive inflation surprises, even though in a low real interest rate setting, it may lead to capital flows to the target zone currency. This mechanism can be amplified by presence of multiple currencies in the target zone with cross-currency constraints on movement versus the target currency (Serrat, 2000).

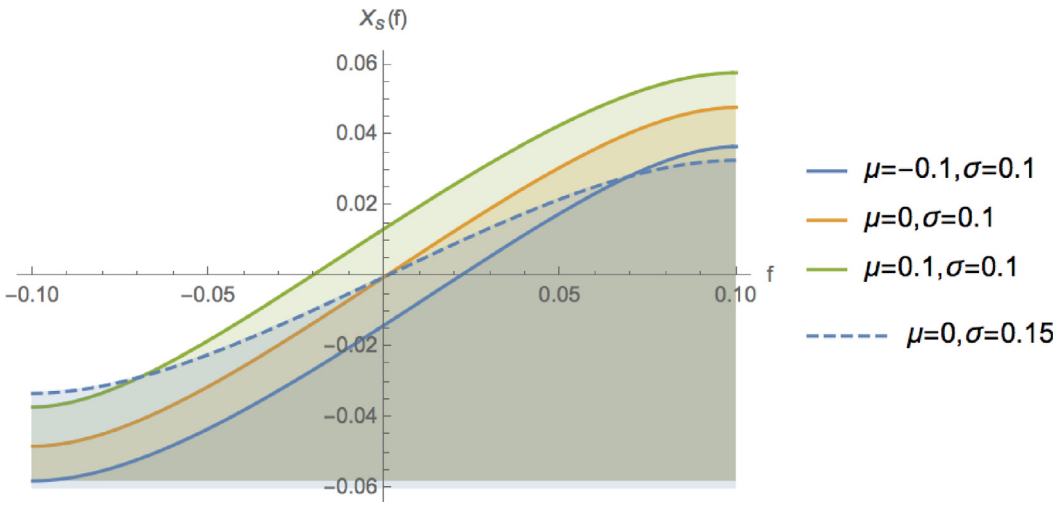

Fig. 12. Mean-reverting stationary dynamics.

cylinder functions. As before, the complete solution is given by an expansion on a complete set of orthogonal functions on the target band, namely:

$$X^*(T-t,f) = X_S(f) + \sum_{k=1}^{\infty} c_k \exp[-(\Omega_k+\alpha)(T-t)]\psi(\Omega_k,f),$$

where the Fourier coefficients c_k again impose the terminal condition $X^*(0,f) = -X_S(f)$. As worked out by Linetsky (2005) explicit though lengthy closed form expressions are obtainable (see Eqs. (39) and (40)). For the case of a symmetric target zone $\underline{f} = -\bar{f}$, an approximation valid for large eigenvalues Ω_k, (i.e. large k's) is given in [L] and reads:

$$\Omega_k = \frac{k^2\pi\sigma^2}{8\bar{f}^2} + \frac{\lambda}{2} + c_0 + O\left(\frac{1}{k^2}\right)$$
$$c_0 = \frac{\lambda^2}{6\sigma^2}(4\bar{f}^2 - 6\bar{f}\mu + 3\mu^2). \tag{37}$$

The normalized eigenfunctions, also up to $O\left(\frac{1}{k^2}\right)$, read:

$$\psi_k(f) = \pm\frac{\sigma}{\sqrt{2}}\bar{f}^{-1/2}\exp\left[\frac{\lambda(f-\mu)^2}{2\sigma^2}\right]\left[\cos\left(\frac{k\pi f}{2\bar{f}}\right) + \frac{2\bar{f}}{k\pi\sigma^2}\phi(f)\sin\left(\frac{k\pi f}{2\bar{f}}\right)\right]$$
$$\phi(f) = \frac{\lambda^2}{6\sigma^2}f^3 - \frac{\lambda^2\mu}{2\sigma^2}f^2 - \left[\frac{\lambda}{2}\left(\frac{\sqrt{2\lambda}}{\sigma}\mu + 1 + c_0\right)\right]f + \theta\mu \tag{38}$$

While strictly speaking Eq. (37) furnishes very good estimates for large k values, a closer look in [L] shows that even for low k's, ($k = 1, 2, \ldots$), acceptable approximations are also obtainable. In particular, for $k = 1$, we approximately have:

$$\tau_{\text{relax}} \simeq [\Omega_1]^{-1} = \left[\frac{\pi\sigma^2}{8\bar{f}^2} + \frac{\lambda}{2} + c_0\right]^{-1}.$$

For these mean-reverting dynamics, the interplay between risk (here solely due to the noise source variance σ^2) and the target band width $2\bar{f}$ on t_{relax} is opposite compared to the DMPS dynamics of Section 2.

The tendency of the fundamental f to revert to its long-run level μ, for a narrow target band, generates an effect of an increase in risk (variance) that is the opposite of the one generated by an increase of β in the DMPS setting, because of the latter's tendency to escape from the mean. If the band is larger, lower levels of σ initially increase the relaxation time, ultimately achieving a decreasing effect. In both cases, an increase in the size of the target band requires a higher T in order for the target zone to be feasible.

Finally, notice that for the O–U case that zero is always the first eigenvalue (which is not surprising, given that it is an ergodic process) and a regime shift is impossible.

Appendix G. Alternative to O–U dynamics: softly attractive drift

We now present the model where we model the fundamental as an ergodic process with a softly attractive drift instead of the Ornstein–Uhlenbeck dynamics. This framework has the advantage of incorporating mean-reverting dynamics while retaining analytical tractability. By "softly attractive" drift we mean the DMPS drift with opposite sign, i.e. $-\beta\tanh(\beta f)$. This model presents similar dynamics to the O–U framework, and allows for a stationary time-independent probability measure. The marginal difference with respect to the O–U dynamics is that the reversion of the fundamental to the mean is softer, and the advantage is that the full spectrum is available and the dynamics do not require an approximation. The equation for the exchange rate after applying Itô's lemma is now given by

$$\partial_t X(t,f) + \frac{1}{2}\partial_{ff}X(t,f) - \beta\tanh(\beta f)\partial_f X(t,f) - \alpha X(t,f) = -\alpha f. \tag{39}$$

Using the equivalent transformation as in the DMPS case, we plug in Eq. (39) into Eq. (20) and obtain:

$$\int^f \cosh(\beta\zeta)\partial_t Y(t,\zeta) + \frac{1}{2}\left[\beta\sinh(\beta f)Y(t,f) + \cosh(\beta f)\partial_f Y(t,f)\right] - \beta\sinh(\beta f)Y(t,f) - \alpha\int^f \cosh(\beta\zeta)Y(t,\zeta)d\zeta = -\alpha f. \tag{40}$$

Now, taking once more the derivative of Eq. (40) with respect to f, one obtains:

$$\partial_t Y(t,f) + \frac{1}{2}\partial_{ff} Y(t,f) - \left[\frac{\beta^2}{2} + \alpha\right] Y(t,f) = -\alpha \frac{f}{\cosh(\beta f)}. \quad (41)$$

Observe now that Eq. (41) is once again equivalent to the standard BM motion case and we can repeat the same procedure we used earlier. The spectrum will now include the eigenvalue zero since we are dealing with a stationary case.

We now proceed as before and Eq. (41) reads:

$$-\partial_\tau Y(\tau,f) + \frac{1}{2}\partial_{ff} Y(\tau,f) - \left[\frac{\beta^2}{2} + \alpha\right] Y(\tau,f) = -\alpha \frac{f}{\cosh(\beta f)}. \quad (42)$$

Consider now the homogeneous part of Eq. (42), namely:

$$-\partial_\tau Y(\tau,f) + \frac{1}{2}\partial_{ff} Y(\tau,f) - \left[\frac{\beta^2}{2} + \alpha\right] Y(\tau,f) = 0.$$

As done before, the method of separation of variables leads us to introduce $Y(\tau,f) = \phi(\tau)\psi(f)$ and the previous equation can be rewritten as:

$$\frac{-\partial_\tau \psi(\tau)}{\psi(\tau)} + \frac{1}{2}\frac{\partial_{ff}\psi(f)}{\psi(f)} - \left[\frac{\beta^2}{2} + \alpha\right] = 0.$$

and therefore we can write:

$$\begin{cases} \frac{-\partial_\tau \psi(\tau)}{\psi(\tau)} = \lambda_k, \\ \frac{1}{2}\frac{\partial_{ff}\psi(f)}{\psi(f)} - \left[\frac{\beta^2}{2} + \alpha\right] = \lambda_k \end{cases}$$

Defining $\Omega_k^2 = \left[\frac{\beta^2}{2} + \alpha\right] + \lambda_k$, the relevant eigenfunction reads:

$$\psi(f) = c_1 \sin(\sqrt{2}\Omega_k f) + c_2 \cos(\sqrt{2}\Omega_k f).$$

Going back to Eq. (20), the boundary conditions at the borders of the target zone $\bar{f} = -\underline{f}$ reads:

$$\partial_f \left[\int^f \cosh(\beta\zeta)\psi(\zeta)d\zeta\right]|_{f=\bar{f}} = 0.$$

which implies that

$$\cosh(\beta\bar{f})\psi(\bar{f}) \quad \Rightarrow \quad c_1 = 0 \quad \text{and} \quad \Omega_k = (2k+1)\frac{\pi}{2\sqrt{2}\,\bar{f}}. \quad (43)$$

We note that Eq. (43) implies :

$$\lambda_k = \frac{(2k+1)^2\pi^2}{8\bar{f}^2} - \frac{\beta^2}{2} - \alpha \geq 0. \quad (44)$$

Lastly, as expected, for the soft attractive case we are able to derive the exact spectrum analytically and unlike in Proposition 2, there is no spectral gap.

References

Ajevskis, V., 2011. A target zone model with the terminal condition of joining a currency area. Appl. Econ. Lett. 18 (13), 1273–1278.

Arcand, J.-L., Hongler, M.-O., Rinaldo, D., 2020. Increasing risk: Dynamic mean-preserving spreads. J. Math. Econom. 86, 69–82.

Arioli, R., Bates, C., Dieden, H., Duca, I., Friz, R., Gayer, C., Kenny, G., Meyler, A., Pavlova, I., 2017. EU Consumers' Quantitative Inflation Perceptions and Expectations: An Evaluation. Technical report, ECB Occasional Paper.

Asmussen, S., Glynn, P.W., 2007. Stochastic Simulation: Algorithms and Analysis, Vol. 57. Springer Science & Business Media.

Bekaert, G., Gray, S.F., 1998. Target zones and exchange rates:: An empirical investigation. J. Int. Econ. 45 (1), 1–35.

Bertola, G., Caballero, R., 1992. Target zones and realignments. Amer. Econ. Rev. 82 (3), 520–536.

Bertola, G., Svensson, L.E.O., 1993. Stochastic devaluation risk and the empirical fit of target-zone models. Rev. Econom. Stud. 60 (3), 689–712.

Bessec, M., 2003. Mean-reversion vs. adjustment to PPP: the two regimes of exchange rate dynamics under the EMS, 1979–1998. Econ. Model. 20 (1), 141–164.

Bossy, M., Gobet, E., Talay, D., 2004. A symmetrized Euler scheme for an efficient approximation of reflected diffusions. J. Appl. Probab. 41 (3), 877–889.

Coibion, O., Gorodnichenko, Y., 2015. Information rigidity and the expectations formation process: A simple framework and new facts. Amer. Econ. Rev. 105 (8), 2644–2678.

Crespo-Cuaresma, J., Égert, B., MacDonald, R., 2005. Non-Linear Exchange Rate Dynamics in Target Zones: A Bumpy Road Towards A Honeymoon Some Evidence from the ERM, ERM2 and Selected New EU Member States. William Davidson Institute Working Papers Series wp771, William Davidson Institute at the University of Michigan.

Dorrucci, E., Fidora, M., Gartner, C., Zumer, T., et al., 2020. The European exchange rate mechanism (ERM II) as a preparatory phase on the path towards euro adoption–the cases of Bulgaria and Croatia. Econ. Bull. Articles 8.

Dumas, B., Delgado, F., 1992. Target zones, broad and narrow. In: Exchange Rate Targets and Currency Bands.

Ferreira, A., Moore, M., Mukherjee, S., 2019. Expectation errors in the foreign exchange market. J. Int. Money Finance 95, 44–51.

Flood, R., Marion, N., 1999. Perspectives on the recent currency crisis literature. Int. J. Finance Econ. 4 (1), 1–26.

Fornaro, L., 2020. Monetary Union and Financial Integration. Economics Working Papers 1677, Department of Economics and Business, Universitat Pompeu Fabra.

Ghosh, A., Gulde, A.-M., Wolf, H., 2020. Currency boards. In: Handbook of the History of Money and Currency. Springer, pp. 687–715.

Gopinath, G., Stein, J., 2019. Banking, Trade and the Making of a Dominant Currency. Working Paper, Under revision for the Quarterly Journal of Economics.

Hansson, A., Randveer, M., 2013. Economic adjustment in the Baltic Countries. Bank of Estonia Working Papers wp2013-1, Bank of Estonia.

Hau, H., Massa, M., Peress, J., 2010. Do demand curves for currencies slope down? Evidence from the MSCI global index change. Rev. Financ. Stud. 23 (4), 1681–1717.

Kac, M., 1966. Can one hear the shape of a drum? Amer. Math. Monthly 73 (4P2), 1–23.

Kalemli-Özcan, e., 2019. U.S. Monetary Policy and International Risk Spillovers. Working Paper 26297, National Bureau of Economic Research.

Krugman, P.R., 1991. Target zones and exchange rate dynamics. Q. J. Econ. 106 (3), 669–682.

Lera, S.C., Leiss, M., Sornette, D., 2019. Currency target zones as mirrored options. J. Deriv. 26 (3), 53–67.

Lera, S.C., Sornette, D., 2015. Currency target-zone modeling: An interplay between physics and economics. Phys. Rev. E 92 (6), 062828.

Lera, S.C., Sornette, D., 2016. Quantitative modelling of the EUR/CHF exchange rate during the target zone regime of September 2011 to January 2015. J. Int. Money Finance 63, 28–47.

Lera, S.C., Sornette, D., 2018. An explicit mapping of currency target zone models to option prices. Int. Rev. Finance.

Lin, H.C., 2008. Forward-rate target zones and exchange rate dynamics. J. Int. Money Finance 27 (5), 831–846.

Linetsky, V., 2005. On the transition densities for reflected diffusions. Adv. Appl. Probab. 37 (2), 435–460.

Lundbergh, S., Teräsvirta, T., 2006. A time series model for an exchange rate in a target zone with applications. J. Econometrics 131 (1–2), 579–609.

Mathieson, D.J., Flood, R., Rose, A., 1991. An Empirical Exploration of Exchange Rate Target-Zones. IMF Working Papers 91/15, International Monetary Fund.

Meese, R., Rose, A., 1991. An empirical assessment of non-linearities in models of exchange rate determination. Rev. Econom. Stud. 58 (3), 603–619.

Mitra, P., 2011. Capital Flows to EU New Member States; Does Sector Destination Matter?. IMF Working Papers 11/67, International Monetary Fund.

Obstfeld, M., 1996. Models of currency crises with self-fulfilling features. Eur. Econ. Rev. 40 (3–5), 1037–1047.

Osler, C.L., 1995. Exchange rate dynamics and speculator horizons. J. Int. Money Finance 14 (5), 695–719.

Rey, H., 2015. Dilemma not Trilemma: The Global Financial Cycle and Monetary Policy Independence. NBER Working Papers 21162, National Bureau of Economic Research, Inc.

Serrat, A., 2000. Exchange rate dynamics in a multilateral target zone. Rev. Econom. Stud. 67 (1), 193–211.
Studer-Suter, R., Janssen, A., 2017. The Swiss Franc's Honeymoon. Working Paper (170), University of Zurich, Department of Economics.
Svensson, L.E.O., 1991. Target zones and interest rate variability. J. Int. Econ. 31 (1–2), 27–54.
Tristani, O., 1994. Variable probability of realignment in a target zone. Scand. J. Econ. 1–14.
Werner, A.M., 1995. Exchange rate target zones, realignments and the interest rate differential: Theory and evidence. J. Int. Econ. 39 (3–4), 353–367.